YEARBOOK OF PHYSICAL ANTHROPOLOGY 39:43–89 (1996)

Shape Analysis Using the Thin-Plate Spline: Neanderthal Cranial Shape as an Example

LUCIA ALLEN YAROCH
STATPROBE, Inc., Ann Arbor, Michigan 48108

KEY WORDS Cranial shape, Neanderthals, Morphometrics, Partial warp analysis, Thin-plate spline

ABSTRACT This paper describes a new geometric method for illustrating and quantifying biological shape difference. The technique is discussed in some detail, and is illustrated by applying it to the problem of characterizing Neanderthal cranial shape. The method of thin-plate splines uses a mathematical model based on the bending of a hypothetical steel plate in order 1) objectively to generate a D'Arcy Thompson–style deformed grid that illustrates the shape contrast between two forms, and 2) to quantify the shape difference by breaking it down into a series of components based on scale. Results confirm the presence of some features traditionally attributed to Neanderthals, but some "classic" Neanderthal features do not in fact characterize the Neanderthal sample. Traits may have been misidentified because of failure to take into account differences in absolute size, use of a misleading frame of reference, and interpretation of one aspect of a large-scale change as a localized feature. In particular, the important Neanderthal "specialization" midfacial prognathism, defined as forward displacement of the nasal region and the tooth row relative to more lateral facial structures, does not appear to be a typical Neanderthal trait. The uniqueness of Neanderthals appears to have been exaggerated, and may be related to Boule's peculiar, flawed reconstruction of the skull of La Chapelle-aux-Saints. The method of thin-plate splines is a powerful technique, capable of providing a new and insightful perspective on morphological problems in physical anthropology.

Physical anthropologists have long been concerned with measurement of biological shape and the quantification of shape differences. Over time, more and more effective methods for this task have become available. Most recently, the field of geometric morphometrics has offered a variety of new techniques, which yield much richer information on shape difference than was possible in the past. One of these techniques, the method of thin-plate splines (Bookstein, 1989, 1991), seems particularly well suited to the kinds of problems commonly approached by physical anthropologists. The thin-plate spline generates useful illustrations of shape difference, and allows one rigorously to address the issue of geometric scale: to ascertain which shape differences are large-scale, involving coordinated changes across broad areas of the form, and which are localized to more limited regions. This article outlines the technique in some detail, using a well known paleoanthropological problem as an example.

The thin-plate spline is one of a series of new geometric techniques for assessing shape difference. Geometric morphometrics goes beyond traditional shape analysis by gaining more information from the landmarks under study. Not only information on chords and angles is included, but information regarding the relative positions of the landmarks is retained as well. Reviewing

geometric morphometrics as a field is beyond the scope of this article. Reviews available in the literature include Rohlf (1990) for a general overview of morphometrics, Bookstein (1991) for extensive coverage of geometric morphometrics using landmark data, and Richtsmeier et al. (1992) for a review of some applications of geometric morphometrics in anthropology. More recent reviews may be found in Bookstein (1996), and numerous examples of the application of geometric morphometrics may be found in volumes edited by Marcus et al. (1993) and by Marcus et al. (1996).

As useful as they may be, accounts of these techniques may seem dauntingly technical to anthropologists who do not specialize in quantitative methods. In addition, the examples used to illustrate the new techniques are often unfamiliar. This article focuses on one new geometric technique, the method of thin-plate splines, and is specifically oriented towards an audience of physical anthropologists, including those who are not well versed in multivariate statistics. The example used to illustrate the technique, Neanderthal cranial shape, is one that is at least somewhat familiar to most physical anthropologists. Rather than reviewing the literature, this article goes more deeply into discussion and illustration of the technique than would be possible in the traditional journal format.

The thin-plate spline has been applied to morphometrics by Bookstein (1989, 1991). This method generates a D'Arcy Thompson–style deformed grid that illustrates shape difference in a very informative way, and also partitions the shape difference into a series of components based on their degree of localization on the form. These components can be quantified, can be related directly to the form under study, and can be illustrated as coordinated movements of landmarks. This approach has been used in zoology (e.g., Tabachnick and Bookstein, 1990; Zelditch et al., 1992, 1993; Swiderski, 1993; Fink and Zelditch, 1995; Zelditch and Fink, 1995, in press; Zelditch et al. 1995; Schaefer and Lauder, 1996) and in physical anthropology (e.g., Albrecht, 1990, 1991; Gelvin and Albrecht, 1993; O'Higgins and Dryden, 1993; Ahlström, 1996).

The article begins with a general overview of geometric morphometrics and the spline model in particular, and goes on to outline the method of thin-plate splines. Two descriptions of the technique are offered. The first one is a relatively simplified version oriented towards a general audience. I apologize in advance to the mathematically sophisticated who may, with some justification, feel I have oversimplified. The second account goes more deeply into the mathematics of the method, and is oriented towards those with a quantitative bent. Those who are uninterested in this degree of mathematical detail should be able to skip over this second more technical description, and still, through the Neanderthal example, get a feeling for what the method does and the ways in which it is useful.

The method of thin-plate splines is illustrated using the Neanderthal example, and some conclusions are drawn about Neanderthal cranial shape, to show the sort of insight that can be gained from a geometric approach. The analysis is limited to two dimensions, but is an exhaustive study—all of the shape information in the landmarks is quantified. Many of the cranial features considered typical of Neanderthals are documented in this analysis. There are, however, some surprising results: some "classic" Neanderthal characteristics seem to be rare to absent in the Neanderthal skulls analyzed here. The skull most commonly used to typify Neanderthals in general, Boule's reconstruction of La Chapelle-aux-Saints does, in fact, show some "Neanderthal" features absent in the others; however, these features disappear in the new reconstruction carried out by Heim (1989). This example illustrates how a reference frame–free approach such as the spline can yield new and surprising insights into a well studied problem.

METHODS

Introduction

This analysis carries out a geometric analysis of cranial shape in Neanderthals. The steps in the analysis are as follows: 1) to separate absolute size from shape difference; 2) to calculate a mean form for each group being compared; 3) to generate a D'Arcy

Thompson–style grid to express visually the shape difference between forms; 4) to quantify shape difference on the basis of scale, i.e., to distinguish between differences involving coordinated change in landmarks distributed broadly across the form from localized differences, in which a few contiguous landmarks change in a coordinated manner; and 5) statistically to compare the Neanderthal partial warp data to modern humans and to representatives of earlier *Homo*.

Geometric vs. traditional shape analysis

Shape analysis has long been of interest to anthropologists and biologists. Karl Pearson was the first to apply multivariate statistics to human craniometric studies. The coefficient of racial likeness (Pearson and Davin, 1924) was Pearson's attempt to quantify differences between modern human populations using cranial measurements. This technique was subsequently modified because it weighted correlated characters. The Mahalanobis D^2 (1936) eliminated the factor of covariance from the calculation of the statistics, and has enjoyed wide use in physical anthropology. Subsequently a number of multivariate statistical techniques became available to anthropologists. Such techniques were the province of the field called multivariate morphometrics (Blackith and Reyment, 1971) or, more recently, traditional morphometrics (Reyment, 1991; Marcus, 1990; Rohlf and Marcus, 1993). In such analyses the variables analyzed are usually chords and angles measured on the forms under study, and commonly an effort is made to identify the shape factors underlying group differences. Examples of such techniques include principal component analysis, canonical variate analysis, and discriminant function analysis. An anthropologist skilled in such techniques is Howells (1973, 1989), who has applied a number of multivariate techniques to craniological problems, and large numbers of anthropologists now use multivariate statistical analysis.

Geometric studies of shape differ from these more traditional approaches in that they allow the original form to be unambiguously reconstructed from the data collected to represent the form, something that is rarely possible using traditional anthropometric linear measurements (Richtsmeier et al., 1992). Using traditional techniques,

> The overall form is neither really archived nor used in the analysis. An investigator may know, for example, that several measurements share a common landmark, but this information is not used in the multivariate analysis. As a result the analyses cannot expect to be as powerful as they would be if that information were taken into account (Rohlf and Marcus, 1993: 129).

In fact,

> The power of biometric methods for broader applications—the fact that discriminant function analysis, for example, works as well in psychiatry as in botany—owes to its discarding half the information of the biometric context, the information that is peculiarly *bio*metric, at the outset (Bookstein, 1992: 20).

Geometric approaches are based on landmark data: landmark positions are recorded in terms of a Cartesian coordinate system, so that each point's (x,y) position can be plotted on a graph. This plot regenerates the original form.

D'Arcy Thompson anticipated geometric morphometrics in his 1917 work *On Growth and Form*. Thompson illustrated shape difference between related animals by superimposing a grid on one and deforming the grid to match landmarks on the second. The deformed grid was a powerful way to illustrate shape difference, but unfortunately the mathematics had not yet developed to allow Thompson to compute the grids objectively—evidently he drew them freehand. Only recently, Bookstein (1989, 1991) has used the mathematics of the thin-plate spline objectively to generate such deformed grids.

Separating shape difference from absolute size difference

The utility of separating shape information from absolute size is widely recognized, both for investigation of relationships between the two (allometry) and to avoid confounding size and shape differences in the analysis. For example, in comparing a 3-foot circle to a 1-foot oval, both the size difference and shape difference between the two are of interest. Any measurement taken on the circle will be affected by its large size. While we are interested in the large size of the circle, it is desirable to isolate size as a single

character, and to analyze the shape difference separately. A circle is a circle no matter how large or small it is, and analyses that separate shape from size attempt to measure this kind of "circleness." The same argument can be made in the comparison of two skulls. The size of a larger individual should be counted only once, if possible, and the shape analyzed separately.

It is of critical importance to make a distinction between *absolute size difference* and *shape difference that is associated with size* (Somers, 1989). The object here is to factor out absolute size while retaining *all* shape difference, including the shape difference which is size-related, or allometry. Allometry may then be studied by correlating shape features with an overall size measure such as centroid size, to document and define the nature of the allometric effect, if any. An example of this approach is the analysis of allometry in piranhas by Zelditch and Fink (1995; Fink and Zelditch, 1995). Thus, ideally absolute size is analyzed separately from shape difference, but shape differences linked to size will remain in the shape comparison.

Shape coordinates

There are a number of traditional multivariate statistical techniques available for dealing with this problem (e.g., Joliceur, 1963; Mosimann, 1970; Mosimann and James, 1979; Darroch and Mosimann; 1985; Somers, 1986, 1989). The field of geometric morphometrics offers new and powerful ways to factor out absolute size. This study uses Bookstein's (1986) shape coordinates for this purpose. This approach involves recalculating the landmark's (x,y) coordinates relative to a baseline defined by two landmarks, according to the following formula (Bookstein, 1991):

$$v_1 = \frac{(x_b - x_a)(x_c - x_a) + (y_b - y_a)(y_c - y_a)}{(x_b - x_a)^2 + (y_b - y_a)^2}$$

$$v_2 = \frac{(x_b - x_a)(y_c - y_a) - (y_b - y_a)(x_c - x_a)}{(x_b - x_a)^2 + (y_b - y_a)^2}$$

Figure 1A illustrates shape coordinates for a series of landmarks on a modern human skull. The shape coordinates are the (x,y) values calculated for landmarks 1–9, 11–16, and 18–20, when 10 is set at (0,0) and 17 is set at (1,0).

These new (x,y) values represent *all* the shape information in a set of landmarks, and so obviate the necessity of selecting a series of chords and angles.

> For small variation in a configuration of any number of landmarks, any ratio of size variables has the same statistical behavior as some linear combination of the shape coordinates of any set of triangles that rigidly triangulates the landmarks (Bookstein, 1991: 137).

This means that if the shape difference is not too great (as in the comparison of cranial shape among members of the genus *Homo*), the shape coordinates include all the information that could possibly be gained from ratios of linear measurements taken from the same landmarks. Since angles can be expressed in terms of ratios of linear measurements, the shape coordinates include all the information in angular measurements as well (ibid).

The statistics of the shape coordinates are independent of the particular baseline chosen if certain conditions are met; that is, the actual (x,y) values of the shape coordinates will differ with different baseline, but the relationships among them will remain the same, as will statistical measures of shape. The statistics of the shape coordinates will be baseline-independent if 1) the forms being compared are not too different; and 2) the shape coordinates for each landmark vary in a circular manner, that is, if the scatter of shape coordinates for each landmark is circular within a sample. Figure 1B shows scatters for shape coordinates in an imaginary sample, from the same view and same landmarks as in Figure 1A. For each landmark the scatter of points illustrates variability in the position of this landmark within the sample. If the scatters are circular, one should draw the same conclusions from an analysis using any alternative pair of baseline points as in the example shown here. In this example all the landmarks have circular scatters except for landmark indicated with an arrow, which has a non-circular scatter. Coward and McConathy (1996) recently compared several methods of shape comparison, including shape coordinates,

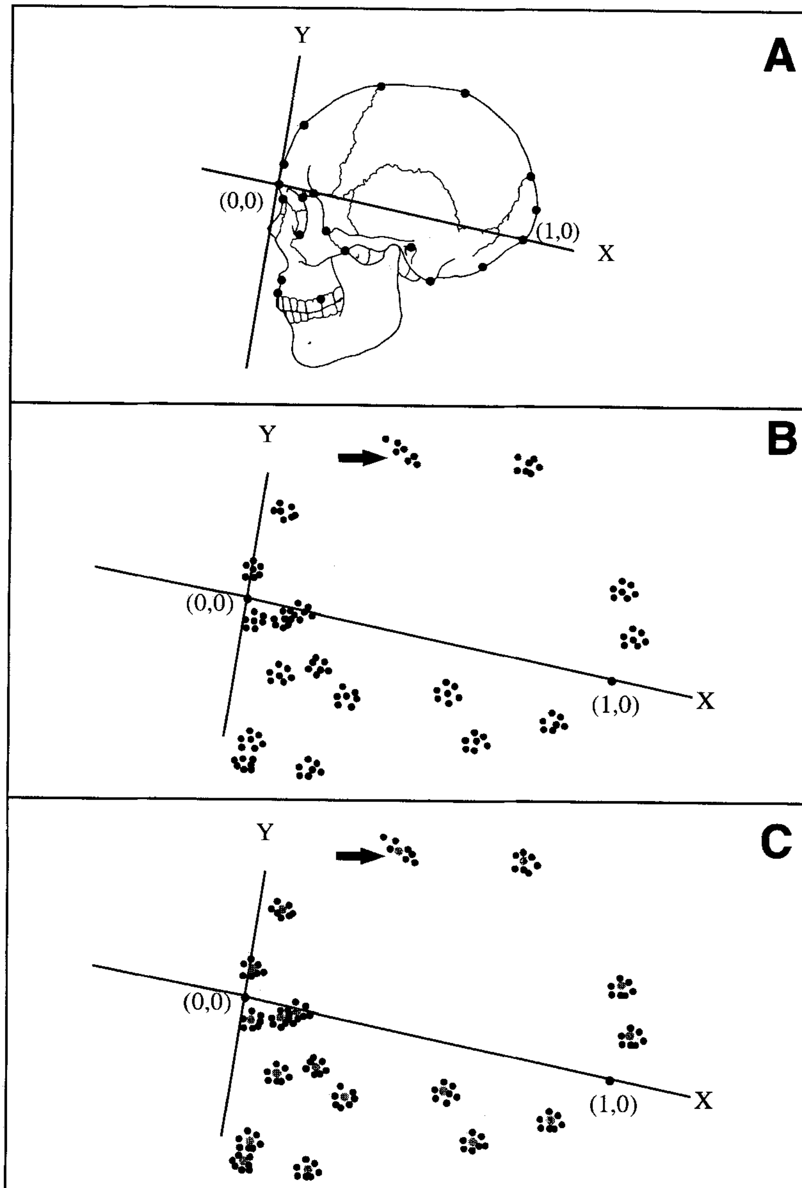

Fig. 1. Shape coordinates. **A:** This illustration shows a series of landmarks on a modern human skull. Bookstein shape coordinates are obtained by recalculating the (x,y) coordinates of each landmark relative to a baseline, with two baseline points set at (0,0) and (1,0) (see equation in text). This procedure factors out absolute size: i.e., if the shape coordinates of several individuals are compared, only shape differences will remain, and absolute size can be dealt with separately. **B:** This plot shows shape coordinate values for several individuals in an imaginary sample, using the same view and same landmarks as in A. For each landmark a scatter of points illustrates variability in the position of this landmark within the sample. If the scatters are circular, then the statistics of the shape coordinates will be independent of the baseline chosen. This means that one should draw the same conclusions from any other pair of points as with the pair shown here. In this example all the landmarks have circular scatters except for the landmark indicated by an arrow, which has a non-circular scatter. **C:** The mean form. The average shape in a sample may be represented by the average position of the shape coordinates for each landmark. The mean position for each landmark is represented by a gray dot. The small dots represent the same scatter of individuals as in B, and illustrate how the individual values vary about the mean.

which they call the Edge Matching Method. They found statistical results from shape coordinate analysis to be baseline-dependent. As the authors themselves point out, their data violate the assumption of circularity, which readily explains why their results were baseline-dependent.

Calculation of the mean form

Shape coordinates offer a straightforward way to compute a mean shape, or mean form, for a sample. Since individual size differences have been removed, what remains is shape difference. The mean form consists of the mean x-value and mean y-value for each landmark across all individuals in the sample: these represent the average position for each landmark, or the average shape. Figure 1C shows the mean form of an imaginary sample of modern humans, using the same landmarks as in 1A and 1B. The scatter of individual data points around the mean illustrates variation in landmark position within the sample.

Incidentally, it is not necessary to use shape coordinates in analysis using the spline (below). The spline itself adjusts for difference in absolute size. The primary role of shape coordinates in this study is that they allow calculation of an average shape for a sample.

Analysis using the thin-plate spline

The thin-plate spline is a mathematical model used in computer graphics that has been applied to morphometrics by Bookstein (1989, 1991). This model is valuable for two reasons. First, it allows one to generate a D'Arcy Thompson–style grid that is an objective result; and second, one can quantify the shape difference by breaking it down into a series of components based on scale. These components can be quantified, can be localized on the form to define precisely what difference is being measured, and the resultant shape features can be analyzed using traditional multivariate statistical techniques.

The spline model. This method models the deformation of one form to another using a mathematical model based on the bending of a steel plate, or spline. (Incidentally, "spline" means thin-plate, so "thin-plate spline" literally means "thin-plate thin plate.") The spline itself is not only imaginary but also has no biological meaning whatsoever. The key feature of the spline model is that it takes more energy to bend the steel plate between landmarks that are close together than it does to bend them between landmarks that are farther apart. Because of this aspect of the plate, the bending energy model allows one to measure shape difference at different scales. The bending of the plate can be used to describe the deformation from one form to another, and the bending itself can be broken down into a series of shape features ranging from large scale to progressively more localized on the form.

Data input for spline analysis begins with a matrix of values for a starting form, or reference form (Rohlf, 1992). The entries of the matrix are derived from the coordinates of the landmarks in the mean form and the interlandmark distances. More information on this procedure is given below. The detailed mathematics of this procedure may be found in Bookstein (1989, 1991). In brief, the spline interpolates the landmark configuration in the reference form to match the landmark configuration in a second form, in a manner that uniquely minimizes the bending of an imaginary steel plate bearing these landmarks. Crudely speaking, one might say this procedure minimizes the deformation of a grid from the reference form to a second form; that is, it deforms the grid as little as possible, by maximizing large-scale change and minimizing localized change.

Total deformation. The total deformation is calculated by deforming a starting form to a second form, using the mathematics of the spline. When coordinate data for a second form is included along with the information in the original data matrix, it is possible to generate a deformed grid that illustrates the transformation of the starting form to the second form. I call this the total deformation in order to distinguish it from deformation associated with specific shape components that represent only a portion of the total shape difference. An example of a total deformation may be seen by skipping ahead to Figure 4, which illustrates the transfor-

mation of the average Norwegian to the average Neanderthal using the landmarks shown in Figure 1A. Such a grid illustrates differences in relative size and position of various parts of the skull. For instance, vertically oriented rectangles (as in the 1–2–3–4 area of Figure 4) indicate relative increase in height of that region and bent areas of the grid illustrate changes in positions of landmarks relative to one another. (In Figure 4, an example of this would be the bend in the grid in between points 4 and 5, which represents a shift in the position of the base of the orbit relative to the jugal point on the zygomatic bone.)

Quantifying shape differences. The shape difference between two forms may be quantified by breaking it down into components based on scale. Large-scale changes are those that involve coordinated change all across the grid, whereas localized changes are confined to some small region of the grid. The spline technique is designed to distinguish between these two. One way this procedure is useful is that it allows one to determine units of analysis objectively. For instance, should the face and the braincase be analyzed separately, or is facial shape linked to neurocranial shape? Another use is in defining characteristics of a form. Is a change in one area a localized characteristic or simply a consequence of a larger-scale change involving landmarks all across the skull? Partial warp analysis allows us to survey the form at various scales to find out whether or not a shape contrast is present at each scale. The spline technique allows us not only to illustrate overall difference between two forms as a deformed grid, but also to represent change at each spatial *scale* as a deformed grid.

Uniform change. There are two kinds of shape change that can be measured for a shape contrast between two forms. The first is uniform (or affine) change, which is the largest-scale possible change. An example of uniform change is shown in Figure 2A as a deformed grid. Uniform change consists of shear, which changes a square to a parallelogram, and stretch, which makes the square taller or shorter. The transformation in Figure 2A shows both: shear, illustrated by the squares becoming parallelograms, and stretch, illustrated by the greater height of the small parallelograms compared to the small squares in the original grid.

Non-uniform change: Principal warps and partial warps. Non-uniform change, in contrast, is expressed differently in different parts of the form. Such change can be large scale, affecting landmarks all across the form, or localized, confined to some small region. We quantify such shape difference using principal warps. The principal warps represent a series of "instruments" for measuring shape contrast at different scales. The number of the principal warps has no scientific meaning, as that number is a direct consequence of the number of landmarks used in the analysis. The number of principal warps is always three less than the total number of landmarks. An example of non-uniform change is the transformation of a square to a kite (Fig. 2B). In this case we have only one principal warp. Use of 15 landmarks would allow measurement of shape differences at 12 different scales, etc. The shape difference at each scale, if there is any, can be illustrated with a deformed grid. Such a grid represents a portion of the warping in the total deformation for the same transformation.

The simplest example of a non-uniform change is the transformation of a square to a kite. This is the only kind of non-uniform change possible in a four-landmark example with a square as the starting form. Square-to-kite transformation is in fact the single principal warp in such an analysis. This warp is characterized by one diagonal of the square moving relative to the other. In the example in Figure 2B we can interpret the change as a shift in landmarks 2 and 4 relative to 1 and 3. While we see non-uniform change in the contrast in Figure 2B, the comparison in Figure 2A would yield no "signal" on the first principal warp, only uniform change. Having four landmarks allows us to measure one component of non-uniform change, but if there is no change at the scale in a given contrast, the "score" for change at that scale will be zero. The scores or signals that may occur at each scale are referred to

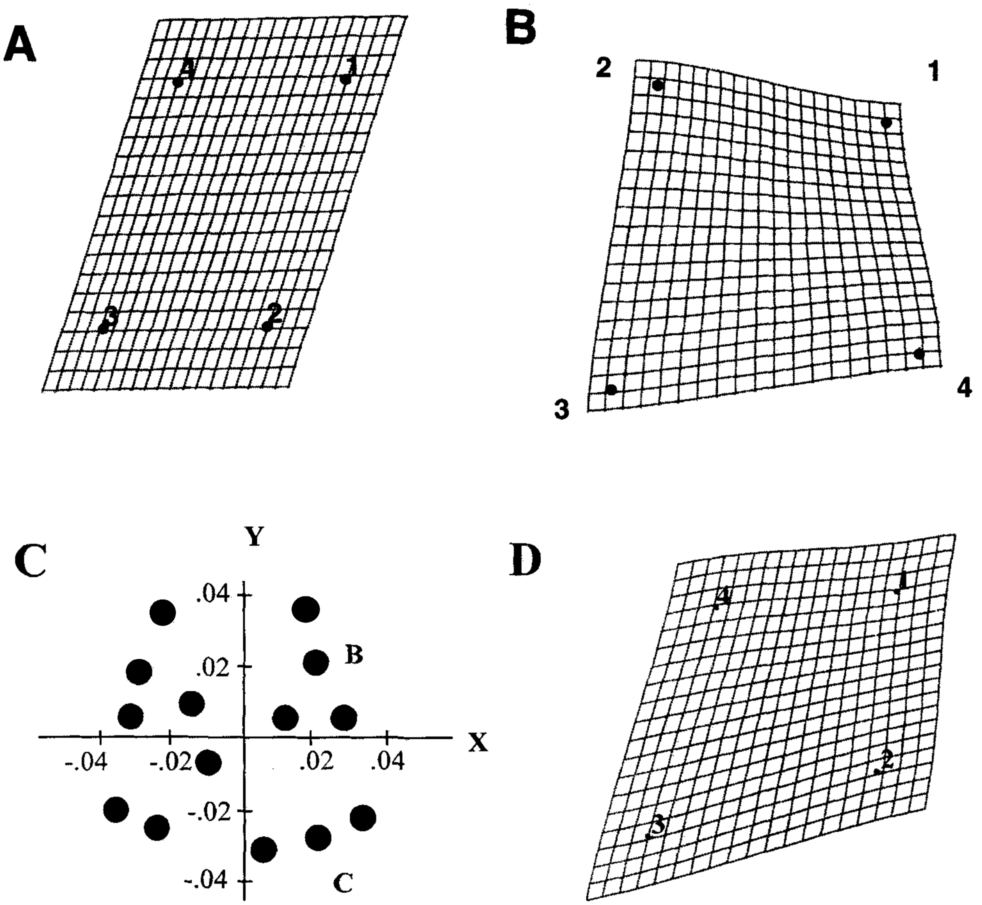

Fig. 2. **A:** Transformation of a square to a parallelogram, an example of uniform shape change. Uniform change consists of (1) shear, which shifts the x-score for each landmark by a distance proportional to its distance from the x-axis, and changes a square to a parallelogram, and (2) stretch, increase or decrease in the value of the y-score making the form shorter or (as in this illustration) taller. Both kinds of change are illustrated in this transformation. **B:** Transformation of a square to a kite: an example of non-uniform shape change. Square to kite is the only kind of non-uniform change possible with only four landmarks. A square to kite transformation is a consequence of one diagonal of a square shifting position relative to the other. In this example, the diagonal from points 2 to 4 has moved up and to the right relative to the diagonal between points 1 and 3. This shift in diagonals, not necessarily obvious in comparison of a square to a kite, is well illustrated by the deformed grid. **C:** Scatter plot of partial warp scores for an imaginary population of quadrilaterals. The square-to-kite transformation is the only non-uniform shape change possible with four landmarks, and characterizes the first (and only) principal warp in a four-landmark comparison. Partial warp scores are multipliers of the principal warp, and indicate the magnitude and direction of change at this scale in a particular transformation. In this scatter plot, the origin represents the reference form, or starting form (in this example, a square), to which each of the others is compared. The distance of each point from the origin represents the magnitude of the shape difference (when that individual is compared to the square), and the orientation of the point relative to the (x,y) axes represents the direction of the change. The partial warp score for the square-to-kite transformation in B is indicated. **D:** This transformation includes both uniform change equivalent to A and non-uniform change equivalent to B. The deformation is the vector sum of the two.

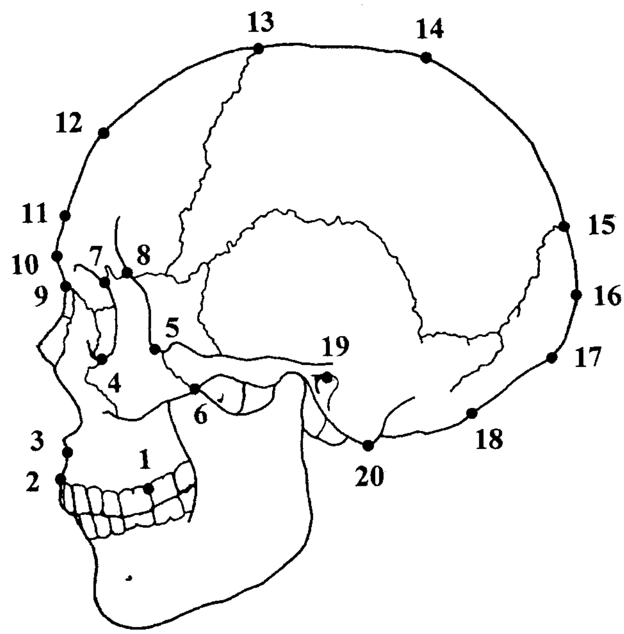

Fig. 3. Landmarks digitized from photographs and scale drawings of crania in *norma lateralis,* shown here on a modern human skull. These landmarks are analogous to traditional anthropometric landmarks, but because they are taken from two-dimensional images, they are not directly comparable. See text for definition of landmarks.

as *partial warps.* A partial warp represents actual shape difference at some particular scale, whereas principal warps are the "instruments" we use to measure them. The principal warp represents some scale we can test for change, whereas its corresponding partial warp represents the change that actually occurs in a given transformation. The partial warp value, expressed as an (x,y) score, quantifies 1) the magnitude of the change and 2) the direction of the change. The partial warp scores for a series of square-to-kite transformations are shown on a scatter plot in Figure 2C. The origin in the plot represents the starting form, and the position of each (x,y) score represents the shape change at this particular scale for some individual. Changes with greater magnitude are more distant from the origin. The direction of change is represented by the position of the point relative to the (x,y) axes—direction referring to the direction of movement of the diagonal of the square. The point B represents the kite in Figure 2B, where 2 and 4 move up and to the right, with 1 and 3 held constant. Point C, on the other hand, describes a kite where 2 and 4 move down and to the right, etc. Commonly, both uniform and non-uniform change occurs in a single transformation. For example, Figure 2D shows a kite which is the vector sum of the the uniform change in A and the non-uniform change in B. Thus, if we began our analysis with the kite in D, we would be able to break it down into the two shape components shown in A and B.

Both the principal warps and partial warps are geometrically independent. For our purposes here, geometrically independent means nothing is being measured twice: change at each scale is factored out before going on to the next-most-localized scale. The scores are called partial warps because, along with the uniform change, they sum to the total warp, or total deformation of the grid. Thus, partial warp analysis consists of

breaking the shape difference in a comparison down into a series of components based on scale. The partial warp score at each scale tells us whether or not change is occurring at that scale, and, if it is, what the direction of magnitude of that shift.

Partial warps are not analogous to principal components. Scatter plots of partial warps represent something very different from scatter plots of components in principal component analysis. Principal components are typically derived from a covariance matrix, and the components are components of variation. Partial warp scatter plots are intrinsically different because they illustrate direction and magnitude of change at a given scale. They have a geometric meaning that can be related to the form under study. In terms of direction, the x-axis corresponds to the orientation of the x-axis in the form under study (in this case the baseline of the shape coordinates). Another baseline would shift the axes, leaving the scatter itself unchanged. It is possible to analyze partial warp data using a procedure analogous to principal components. These components are called relative warps (see Bookstein, 1991; Tabachnick and Bookstein, 1990), and will not be discussed in this article. Note also that the eigenvectors and eigenvalues have a different significance than those in a principal components analysis. With the spline, the eigenvectors of the bending energy matrix are the principal warps (see below). Their eigenvalues are inversely proportional to the spatial scale of the shape difference measured by that warp. Thus an eigenvalue has nothing to do with the importance of that warp in explaining the shape difference, but everything to do with the scale of the shape difference it quantifies.

Statistical comparison of partial warps. The next step in analysis after calculating and scattering partial warps is to determine which shape components show an interesting difference between two forms or two groups, i.e., at what geometric scale(s) do the two differ? For a comparison of one partial warp in two samples, the Hotelling's *t*-squared is used. This test is analogous to a Student's *t*-test, testing for the significance of difference between means, but allows one to compare the x and y scores for a partial warp in a single procedure. This is appropriate because the x and y scores together describe a single contrast.

More complete description of the method. This method models the deformation of one form to another using a mathematical model based on the physics of bending a thin plate of steel. Landmark displacements in the x-y plane are modelled as though they were vertical displacements of an infinite, uniform, infinitely thin metal plate tacked at given heights above the landmarks of the starting form. The surface of this plate, or spline, is mathematically described by a function that minimizes the energy needed to bend the plate. The bending of the plate can be used to describe the deformation from one form to another, and the bending itself can be broken down into components based on degree of localization, thus describing and quantifying the difference in shape between two forms as a series of components ranging from large scale to progressively more localized on the form.

The set of descriptors for a shape comparison depends on the reference form. From the starting form a thin-plate spline is calculated, based on all the interlandmark distances and a certain function U(r).

$$z(x,y) = -U(r) = -r^2 \log r^2$$

(See Bookstein, 1991, for a full technical explanation of the mathematics and geometry of this procedure.) The thin-plate spline is calculated based on a matrix of values U(r), where the r's are all of the interlandmark distances for the starting form, and based on the (x,y) coordinates for each of these points. Using the coordinates of a second form, a spline can be calculated that interpolates the correspondence of each landmark in the starting form to the homologous landmark in the second form, the vertical displacement at each point representing the actual displacement in the (x,y) plane.

The deformation from one form to another can be conceived of as though the starting form were printed on a transparent sheet of

plastic and then bent into a position that puts the shadow of each landmark over the landmark location of its homologue in the second form (Zelditch et al., 1992). The thin-plate spline for the total deformation is a four-dimensional one, because a three-dimensional spline cannot express both x- and y-shifts at the same time. Two "verticals" are necessary, one to represent x-displacement in the two-dimensional plane, and one to represent y-displacement. It can be visualized as a three-dimensional spline only when displacement is limited to the x- or the y-direction, as in a square-to-kite transformation. For example, in the transformation in Figure 2B, picture the y-axis is connecting points 1 and 3 and the x-axis connecting points 2 and 4. The spline models this deformation: if the vertical displacements are flipped 90 degrees and added to the y-coordinates of the original square, the result is Figure 2B. Downward displacements in the spline are subtracted from the y-coordinates and upward-displacements are added, yielding a deformation of the starting form, the square, to the second form, the kite. As mentioned above, a transformation involving both x and y shifts requires either a four-dimensional spline or two splines to illustrate the shift, one for the x-component and one for the y-component.

Following the shadow analogy above, the manipulation of the plastic sheet to model the second landmark configuration involves both tilting and bending of the sheet to orient the shadows of the landmarks. The tilting of the sheet, or spline, is analogous to the uniform change, change where parallel lines remain parallel, as in the square to parallelogram transformation in Figure 2A. In a uniform transformation, "if a rectangular grid were superimposed on the form, every small square of this grid would be transformed to the same parallelogram in the same orientation" (Zelditch et al., 1992: 1168). In non-uniform change the landmark configuration deforms more in some parts of the form than in others, as in the deformation of square to kite (Fig. 2B, above). Any deformation is the sum of its uniform and non-uniform components.

Using the model of bending of a steel plate, the calculation of the thin-plate spline for a particular transformation allows interpolation of the configuration in one form to the configuration to the second "in a manner that *uniquely* minimizes a certain sort of 'bending energy,' namely, the (linearized) energy that would have been required had the landmark displacements in question been normal to the plane of the figure rather than within that plane" (ibid: 31, emphasis in original). The bending energy model is particularly useful in that it can be used to separate the shape change in the deformation from one form to another into components based on degree of localization on the form. It takes more energy to bend the plate between landmarks that are close together than between landmarks that are far apart. A *bending energy matrix,* based on the function U(r) of the interlandmark distances and the coordinates of the starting form, generates a series of eigenvectors, the *principal warps,* that can be used to describe a series of patterns of shape change, ranging from large scale to more and more localized deformation. Note that the bending energy matrix is calculated solely from information from the reference form, and thus is completely a function of the reference form itself, and not of any particular second form that is being compared. The number of principal warps is three less than the number of landmarks: in the following study of 20 landmarks, there are 17 principal warps. The number of features of shape change thus depends on the number of landmarks used—the more landmarks used, the more principal warps, and the more detailed the information on degrees of localization that may be obtained. Thus the bent principal warps are the descriptors of the non-uniform change only. The bending energy matrix has three zero eigenvalues which correspond to uniform change (Bookstein, 1991), while the other non-zero eigenvalues match the bent principal warps.

Each principal warp is expressed as a series of coefficients, as many as there are landmarks in the analysis. "Each eigenvector can be visualized, and understood, as a pattern of bending (= deformation), a shape change that is distinctive by virtue of having a well-defined geometrical scale and

'center' " (Bookstein, 1991: 322). The principal warps themselves can be represented as thin-plate splines, with vertical displacement at each landmark proportional to the coefficient for that landmark. Positive coefficients represent upward shift of the landmark, negative coefficients, downward shifts. The spline for the square-to-kite transformation is also the spline for a principal warp: with four landmarks only one principal warp can be defined and the total non-uniform change is expressed as a single non-uniformity. Any square-to-kite transformation can be described by some vector multiple of this spline. These vector multiples are called the *partial warps*.

While the principal warps represent potential ways the starting form can change, the partial warps represent the actual change in a particular transformation of the reference form to a second form. Each partial warp is a 2-vector multiple of the principal warp, a multiple by some (x,y) score. Each coefficient of the principal warp is multiplied by the (x,y) values of the partial warp to give a magnitude and direction to the landmark shifts implied. While the spline for a square is a principal warp, the actual transformation to a particular kite (Figure 2B is an example) is a partial warp. The spline for a square can, with the appropriate vector multiplier, be used to describe any square-to-kite transformation in any orientation and to any degree. Each partial warp is a projection of the three-dimensional principal warp into the two-dimensional (x,y) plane.

The shadow analogy for the spline may also be applied to the principal warps: a shadow from the spline expresses different square-to-kite transformations depending on the location of the light source. A light source directly above the spline will orient the shadow directly over the original landmarks, producing no change in landmark position, while a lower light source will produce a "shadow" and thus a set of landmark displacements. The partial warp (x,y) coefficients determine the "position" of the light source, both its height and its angle of approach.

Thus the partial warp coefficients can be used to describe magnitude and direction of change at the particular degree of localization described by the matching principal warp. After uniform change, under which all shifts are parallel and proportional to some original coordinate, the first few principal warps describe the largest scale changes, those in which the landmarks are moving together to the greatest degree. The more localized warps shift landmarks in one area a great deal, whereas more distant landmarks shift very little. For each partial warp all the landmark displacements are parallel to one another, the orientation determined by the partial warp vector score (x,y). The relative distances of displacements of the landmarks are a function of the principal warp coefficients, landmarks with negative coefficients moving in the opposite direction to landmarks with positive coefficients.

The uniform change and the displacements from all the partial warps sum to the total deformation for any particular transformation. An exhaustive description of the shape difference between two forms, they parcel the shape difference into a series of components based on degree of localization. These components can be quantified and analyzed statistically to obtain an objective description of the shape difference in any comparison, of the shape variation in any sample, or of the differences among samples.

Neanderthal cranial shape and the thin-plate spline

The method of thin-plate splines will be illustrated by applying it to a problem at least somewhat familiar to most physical anthropologists: description of Neanderthal cranial shape. The skull is an important source of data in discussions of the "Neanderthal Problem," that is, the ongoing debate regarding the fate of Neanderthals and their role in the evolution of modern humans. According to one perspective, Neanderthals differ from more modern humans primarily in having larger muscles, faces, and teeth, particularly the anterior teeth (e.g., Brace, 1995; Smith and Paquette, 1989), and a number of researchers believe that Neanderthals were ancestral to some modern populations (e.g., Brace, 1995; Frayer, 1992; Wolpoff, 1992). At the other extreme are those who see the Neanderthals as fundamentally different from ourselves. These authors at-

tribute to the Neanderthals a series of highly unique features, distinguishing them both from non-Neanderthal populations contemporary with them and from all later humans; they further argue that modern humans share a more "generalized" or primitive morphology with earlier *Homo* (Howells, 1974; Santa Luca, 1978, 1980; Stringer et al., 1984; Rak, 1986, 1992). On this basis, they argue that the Neanderthals made little (Braüer, 1992) or no (e.g., Stringer and Andrews, 1988; Vandermeersch, 1989; Rak, 1992) genetic contribution to later populations.

The Neanderthal example seems particularly suitable for illustrating the spline approach, because 1) Neanderthal cranial shape is well studied, so results from spline analysis can be compared to the consensus derived from more traditional approaches; and 2) there remain some disagreements about the nature of some shape features of Neanderthal skulls, despite the fact that all researchers are studying the same limited sample of crania. Description of one of the most important features in Neanderthals, midfacial prognathism, is dependent on frame of reference (see below). Thus a reference-frame free approach should be particularly informative. The spline technique is applied to Neanderthal cranial shape both to illustrate the technique and to investigate aspects of Neanderthal cranial shape. Data generated by the spline attempt to document the presence of shape features traditionally ascribed to Neanderthals.

Numerous characterizations of Neanderthal cranial shape are available in the literature (e.g., Schaaffhausen, 1858; Huxley, 1863; Schwalbe, 1901; Sollas, 1908, Boule, 1911–1913; Hrdlička, 1930; McCown and Keith, 1939; Coon, 1962; Brace, 1964, 1979; Howells, 1973, 1974; Heim, 1976; LeGros Clark, 1978; Wolpoff, 1980; Wolpoff et al., 1981; Smith, 1983; Trinkaus, 1983, 1984, 1987; Trinkaus et al., n.d.; Rak, 1986; Hublin, 1978; Smith and Paquette, 1989; Spencer and Demes, 1993). It is generally agreed upon that Neanderthals are characterized by a long, low cranial vault with a protruding occiput and low forehead, and a large, tall face with big orbits and a large, continuous supraorbital torus. The midface is projecting: associated features include the large, projecting nose, flat and retreating zygomatic arches, the absence of a canine fossa, lack of a chin, and a gap behind the mandibular third molar (called the retromolar space).

Midfacial prognathism is considered one of the most distinct Neanderthal features. Coon (1962) argued that the forwardness of the Neanderthal midface was a consequence of the marked projection of the nose, with the anterior position of the dentition being a secondary consequence of nasal projection. Wolpoff et al. (1981) quantify this kind of prognathism by measuring the projection of nasion anterior to a bifrontomalarorbitale line. Howells (1973) agrees that the nasal region projects in Neanderthals. He also cites simultaneous retraction of the malar and forward placement of the teeth as a major Neanderthal character (Howells, 1974). He emphasizes the presence of the retromolar space in the mandible as evidence of facial forwardness. Forwardness of the nasal region and the tooth row is evaluated relative to the zygomatic region (Trinkaus and Howells, 1979).

Heim, however, argues that Neanderthals are not prognathic in the way the term is commonly used in describing modern humans.

> . . . facial volume in La Ferrassie 1 is not the consequence of prognathism at all, as previously believed, but the geometric expression of a product of the three dimensions (length, height and width) which attain more elevated values in La Ferrassie than in the other Neanderthals or in modern humans (Heim, 1976; 190; my translation).

Smith and Paquette (1989) agree that facial prognathism in Neanderthals is related to their large facial size as opposed to a shift in position of one or more portions of the face. Citing the human craniofacial growth literature, they point out that as the human face grows it is displaced in an anteroinferior direction rather than straight downwards. Thus, increase in facial height would involve obligatory increase in horizontal facial dimensions and facial projection. In contrast, Rak (1986) attributes the midsagittal projection of the Neanderthal face to a parasagittal shift in the orientation of the *infraorbital*

plate. He argues that this feature would resist rotation and torsion of the anterior part of the face during heavy use of the anterior teeth. Trinkaus (1984, 1987), on the other hand, explains midfacial prognathism as a consequence of a retreat of the cheek region, in comparison to earlier *Homo*. Spencer and Demes (1993) explain prognathism in Neanderthals in terms of shifts in the relative positions of the anterior and posterior dentition and the anterior attachments of the masticatory muscles. They argue that the Neanderthal arrangement would provide a longer moment arm for both incisal and molar biting.

How are we to evaluate these different characterizations of Neanderthal midfacial prognathism? Some of them are difficult to compare one to the other because their definitions are reference-frame specific. For instance, two hypotheses proposed to explain Neanderthal facial shape focus on the position of the masticatory muscles. Trinkaus (1987) argues that in Neanderthals the anterior attachments for masseter and temporalis shift *posteriorly* relative to the dental arcade in comparison to earlier hominids. Alternatively, according to Spencer and Demes (1993), both the masticatory muscles and the molar teeth are located more *anteriorly* relative to the temporomandibular joint. Using the thin-plate spline, I was able to show that these two competing hypotheses are mutually compatible (Yaroch, 1994b). I was able successfully to compare these two hypotheses because the thin-plate spline technique is reference-frame free: the position of each landmark is evaluated relative to *all* other landmarks rather than a single point, line or plane. Thus, this approach is particularly suited to addressing issues such as the nature of Neanderthal prognathism.

In this study, cranial shape in Neanderthals is compared to a series of more recent human cranial samples and to the earlier hominids Petralona and Kabwe. Shape comparison is based on a series of 20 landmarks digitized from photographs and scale drawings of the skull in a lateral view. The analysis seeks to define and quantify features of cranial shape that distinguish Neanderthals from more recent humans and from the two earlier hominid crania.

Sample. In this study, the term "Neanderthal" refers to fossil humans from the Near East and Europe dating from less than 100,000 to approximately 35,000 years BP that combine fully modern brain size with the relatively large face characteristic of earlier humans. This group is sometimes referred to as the "classic Neanderthals." For all samples, I included only adult crania identified as male by an experienced researcher. Disproportionate representation of the sexes in a combined sample could bias results, and the available female cranial sample for Neanderthals is too fragmentary to allow a separate analysis. I included all the adult male Neanderthal crania complete enough to preserve most of my landmarks: La Ferrassie 1 (Heim, 1976, Pl. I), Guattari 1 (Piperno and Schichilone, 1991, average of Pls. I and II), Amud 1 (Suzuki and Takai, 1970, Pl. XX), Shanidar 1 (Trinkaus, 1983, Fig. 9), and La Chapelle-aux-Saints, both Boule's original reconstruction (1911, Fig. 24), and Heim's more recent reconstruction (discussed in Heim, 1989; cranial data for the new reconstruction taken from a photograph kindly provided by Dr. Erik Trinkaus).

My comparative material includes five recent human samples. I tried to represent modern human variation as completely as possible given the availability of high-quality photographs or scale drawings in the literature. I included Norwegians (Schreiner, 1939; N = 44), Ugandans (Gornv, 1957, N = 34), Greenland Eskimos (Fhrst and Hansen, 1915, N = 25), Australians (Berry and Robertson, 1914, N = 28), and Polynesians (von Luschan, 1907, N = 25). All of these samples were photographic except for the Australian sample, which consisted of dioptrographic drawings.

Two Middle Pleistocene hominids, the Petralona and Kabwe crania, are included in the analysis. Landmark data are taken from the photographs in Thorne and Wolpoff (1981, Fig. 1). These individuals are assigned to different species by different authors, including *Homo erectus* (e.g., Coon, 1962; Brace, 1991), early archaic *Homo sapiens* (e.g., Stringer et al., 1979; Wolpoff, 1980: Groves, 1989), and *Homo heidelbergensis* (Rightmire, 1990), or to an *H. erectus* to *H. sapiens* transition (Brace, 1995). These cra-

nia are chosen as relatively complete representatives of earlier *Homo* and their specific designation is not of critical importance for this analysis.

Landmarks. Analysis of shape difference is based on a series of 20 landmarks digitized from photographs or scale drawings of crania in *norma lateralis* (shown on a drawing of a modern human skull in Figure 3). Thus the data in this study are limited to the two-dimensional representation of a three-dimensional object. The lateral view was chosen because all lateral images are taken with comparable orientation of the skull as (opposed to *norma frontalis,* where a standard orientation is necessary), and because more of the features thought to be important in the Neanderthal cranium are represented in *norma lateralis* than in any other single view. Examples of these features include relative proportions of the face and neurocranium, midfacial prognathism, brow projection, forehead profile, and occipital protrusion.

Choice of landmarks is a compromise between 1) covering the form as completely as possible and 2) choosing landmarks that are readily recognizable in lateral images, and are preserved in the largest number of individuals possible. A pilot study was carried out on a series a of modern skulls in the Laboratory of Physical Anthropology at the University of Michigan. I compared inter-landmark distances calculated from digitized lateral photographs to chords measured on the original skulls. Correlations between the two were very high for almost all the landmarks investigated. An exception was asterion, which is easy to misidentify on lateral photographs; thus this landmark is not included in the 20 used here. Some other landmarks were dropped because they are so rarely preserved in fossil crania. This pilot study does not test the effects of photographic distortion, as I took the photographs myself using a telephoto lens at a distance of 8 feet, which essentially eliminates distortion. With published photographs I do not have control over these factors, so distortion remains a potential source of error in the analysis below.

While the landmarks do not explicitly include information on the curving of form between them, "in practice they seem to include enough of that information to fairly represent the statistics of the curving" (Zelditch et al., 1992). The majority of the landmarks represent homologous points, but some non-homologous landmarks are included, primarily extremes of curvature on the neurocranial outline, better to represent the whole of the cranial contour. These landmarks are called deficient landmarks because they lack one coordinate (see Bookstein, 1991). The landmarks are defined as follows.

1. Point on the alveolar margin at the junction of the first and second molars; if a gap was present in this area the point was taken halfway between the two teeth.

2. Approximation of prosthion; the most anterior and inferior point visible on the maxilla.

3. An approximation of nasospinale, taken below the nasal spine.

4. Approximation of orbitale taken as the most inferior visible point on the margin on the orbit.

5. Jugale—a point on the zygomatic bone, the "corner" where the lateral orbital pillar and zygomatic process meet.

6. The most inferior point on the temporozygomatic suture in lateral view.

7. An approximation of frontomalarorbitale; the most anterior point on the zygomaticofrontal suture visible in lateral view.

8. An approximation of frontomalartemporale; the most posterior point on the zygomaticofrontal suture visible in lateral view.

9. Approximation of nasion; most anterior point on the frontonasal suture visible in lateral view. This point will not be identical to true nasion, particularly in asymmetric individuals.

10. The most anteriorly projecting point in the brow region (most distant from a line perpendicular to the Frankfurt horizontal). This point is similar to glabella but will be more anterior when the brow ridge projects more than the midline (as it commonly does).

11. Approximation of supraglabellare; the point in the region above the brow ridge most distant from a line between points 10 and 12. This is a deficient landmark.

12. Approximation of metopion; point on

the frontal contour most distant from a line between points 10 and 13; another deficient landmark.

13. Approximation of bregma; the most superior point on the coronal suture visible on the image. Tends to be located slightly lateral to the midline and anterior to true bregma.

14. A deficient landmark consisting of the point on the mid-parietal contour most distant from a line connecting points 13 and 15.

15. Approximation of lambda: the point where the lambdoid suture crosses the skull outline in a lateral view; frequently slightly lower than true lambda. If an extrasutural bone is present at lambda but not visible in norma lateralis this point is included in the analysis even though true lambda may be difficult to define.

16. A deficient landmark defined as the point most distant from a line from 15 to 17; often coincident with opisthocranion.

17. A landmark similar to inion, defined as the point where the occipital and nuchal planes meet as seen in lateral view.

18. A deficient landmark on the nuchal plane defined as the intersection of the skull outline and a perpendicular dropped from the midpoint of a line between 17 and 20.

19. An approximation of porion: the most superior point on the border of the external auditory meatus.

20. An estimate of mastoidale: the point at the tip of the mastoid process as seen in lateral view.

For simplicity the traditional landmark names, such as prosthion, orbitale, glabella, etc., will be used to refer to these landmarks in the text, even though many of them are only approximations of the standard anthropometric landmarks. This system of landmark definition is internally consistent, but because they are defined differently, these landmarks are *not* comparable to bregma, lambda, etc., on lateral craniographs or radiographs.

Estimation of missing data. Several fossil crania included in the analysis were missing data for one or more points. In these cases, the preserved landmarks were digitized and included in the calculation of the mean form of the appropriate sample. In order to analyze specimens as individuals, however, complete data are necessary. No landmarks were estimated for the modern samples, but for four of the Neanderthals and for Petralona missing data were estimated to obtain information on individual variation. Estimated data were not included in the calculation of the mean form. Data estimation was carried out using the thin-plate spline (see below), based on the sample mean configuration. For the Neanderthals the following landmarks were estimated for individual analysis: Guattari, Points 1 and 2; La Chapelle, Point 1; La Ferrassie, Point 6; and Amud, Point 6. Point 20 in Petralona was estimated based on Kabwe's configuration.

One advantage of using the thin-plate spline is that it offers a new way to estimate missing data that incorporates all available landmark information. Using the TPSpline program, the group mean form is deformed into the configuration for the individual in question, but the landmark(s) to be estimated are ignored, so that the deformation is calculated solely on the basis of the points actually represented; that is, the missing landmark is turned off, and a deformed grid calculated from the remaining 19. The point to be estimated is "dragged along" in the deformation, so that a new position is attained. Thus the estimated landmark is located using all the information in the landmarks preserved.

The estimated location of the landmark is based on the group mean location as modified by the particular individual configuration. Since the Neanderthal mean form is the starting form for this deformation, any error will make the individual's shape more similar to the mean than it was in reality; no spurious information will be added, as may occur when estimation is based on few landmarks. In other words, any error will be in the direction of making that individual "less bent away" from the mean, thus potentially reducing the variability in shape but avoiding the addition of false information. This approach permits inclusion of incomplete specimens in partial warp analysis for individuals, where complete data are necessary, without inserting erroneous information.

Steps in the current application

Shape coordinates and calculation of mean forms. Landmark data were converted to shape coordinates using a glabella-inion baseline (landmarks 10 and 17). It is appropriate to use shape coordinates because 1) skulls belonging to the genus *Homo* are similar enough to compare using shape coordinates (Bookstein, personal communication), and 2) the scatter of the shape coordinates within the Norwegian reference sample is circular for all 20 landmarks (including even the deficient landmarks). Mean forms were calculated from the shape coordinates for the Norwegian and Neanderthal samples (Fig. 4). Kabwe and Petralona were not averaged but were analyzed separately.

In my original study (Yaroch, 1994a), I computed the Neanderthal mean from all five Neanderthal crania, including La Chapelle-aux-Saints. La Chapelle was represented by Boule's reconstruction because a good lateral photograph of Heim's new reconstruction was not available in the literature. It was immediately apparent that La Chapelle differed markedly from the other Neanderthals in several features (Yaroch, 1994a, 1995, n.d.); thus its inclusion for calculation of the Neanderthal mean form was questionable. Recently, because Dr. Erik Trinkaus generously made a photograph available to me, I have been able to add the new reconstruction of La Chapelle to the analysis. Comparison of the two reconstructions is very informative; however, there is some question as to whether the new photograph is in a true lateral orientation (see below). Thus in this analysis I include discussion and comparison of the "new" La Chapelle, but calculate the mean form from the other four Neanderthals.

The Norwegian mean form is used as reference form: partial warps are based on a series of principal warps derived from the Norwegian mean form. Results would have been similar had the Neanderthal mean been used. I use the Norwegian mean because it is based on a true sample with N = 44, as opposed to the Neanderthal mean which is based on only a few, reconstructed individuals. For partial warp data, the scatter of individuals about the Norwegian mean gives a feeling for how a human population varies in such traits. Then the Neanderthal values can be evaluated with the perspective of this scatter. In some cases alternative starting forms are used to illustrate a contrast between two forms. Any starting form can be used to compute a total deformation. To generate comparable partial warp data, however, all partial warps are based on transformation from the Norwegian mean form.

Individuals from the other modern samples are included on the scatters of partial warps to get a better idea of variation in modern *Homo sapiens*. Inclusion of these additional samples allows one to distinguish shape features where the Neanderthals differ from features where the Norwegians diverge both from Neanderthals and from other modern populations. Partial warp results for the Ugandan, Australian, Polynesian, and Eskimo mean forms are not included here, nor are these samples individually identified on the scatter plots; this is because they make the scatter plots overly complicated and difficult to interpret. Total deformations and partial warp data for the mean forms are included in the partial warp analysis in Yaroch (1994a). This reference also includes scatter plots where Ugandan, Eskimo, Polynesians, and Australian individuals are labelled separately.

Spline analysis was carried out on a personal computer using the program TPSpline (Rohlf, 1990), which generates principal warps for the starting form, computes and illustrates the Cartesian deformation of the starting form to each mean or specimen analyzed, and calculates the partial warps for each comparison. Use of 20 landmarks in this study allowed the shape difference to be broken down into 18 features, the uniform factor and 17 non-uniform degrees of localization for each comparison made. Partial warp coefficients were uploaded to the University of Michigan's mainframe computer and analyzed statistically using the Michigan Interactive Data Analysis System (MIDAS).

RESULTS

Total deformation

In this section I describe the total Cartesian deformations of the starting form to the Neanderthal mean, to Petralona, and

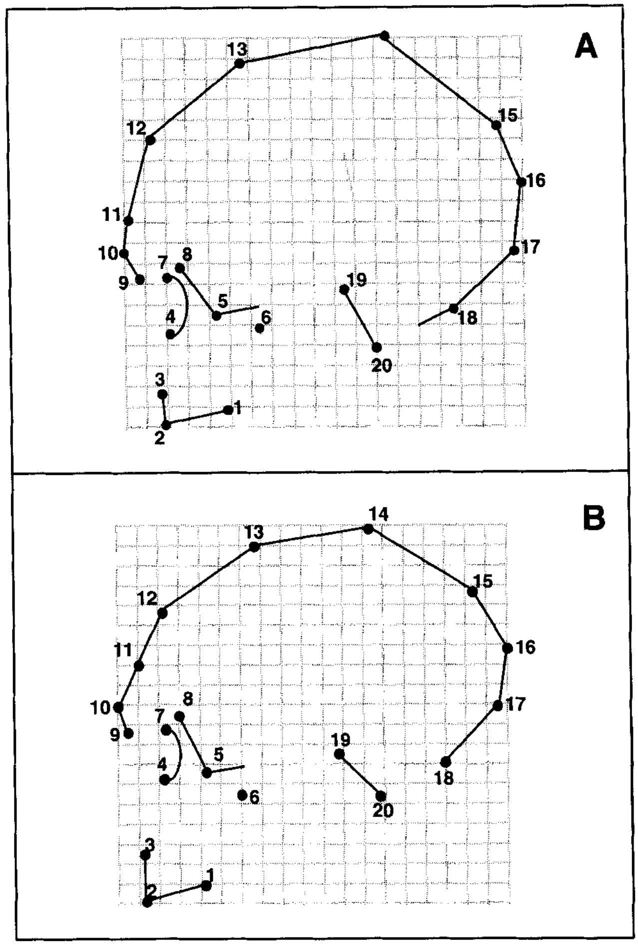

Fig. 4. Mean forms for (**A**) the Norwegian and (**B**) the Neanderthal samples. Calculated using Bookstein shape coordinates, shown on undeformed grids. Each point shows the average location of that landmark in the sample, after the effect of absolute size is removed. The lines connecting the landmarks are provided only to aid in interpretation of the figure, and do not represent data included in the analysis.

to Kabwe. It should be noted that, in this portion of the analysis, these transformations will be made in the direction opposite to evolutionary time: the Norwegian mean will be deformed to the fossil configurations, and not vice versa. These deformations will all be "backwards" because a mean used as reference form should be based on a larger sample size than is available for fossil groups. In the following descriptions, all terms referring to shape *change,* such as reduction, increase in size, and any other movement of landmarks, are only aspects of this description as deformation and do not pertain to any evolutionary process unless specifically indicated. These comparisons are made with the effect of size completely removed, such that *all* "increase in size" or "reduction" is a *relative* change, i.e., a change in proportion.

As discussed above, the deformation of the grid seems to represent change between the landmarks quite well (Zelditch et al., 1992). Localized shape contrasts that are unrepresented by landmarks here will not be represented in the total deformation. Inasmuch as changes in unrepresented regions are coordinated with the 20 landmarks used here,

they will be represented accurately in the total deformation. For the braincase in particular the landmarks used should be quite representative, since these bones are predominantly smooth and have few landmarks anyway. Inclusion of landmarks at the junction of the frontal, parietal, and occipital bones with the temporal would have allowed fuller representation of braincase shape, but these landmarks were excluded for practical reasons (see above). Thus descriptions about what is happening to the "parietal region," "occipital region," etc., specifically refer to the deformed grid, not necessarily to the Neanderthal skulls themselves. However, examination of casts of Neanderthal skulls confirms that the grid represents overall form very well, just as predicted by Zelditch et al. (ibid.).

Please recall that the purpose of these deformed grids is to *illustrate* the shape contrasts between two forms. These differences will naturally be visible in a comparison of the starting form to the second form, without deformation. However, many differences that are unlikely to catch the eye in an undeformed comparison are very clear on the deformed grid. Thus, individual configurations of Petralona and Kabwe will be shown only on the grid deformed from the Norwegian mean. Each landmark configuration is identical on deformed and undeformed grids, so presentation of each on an undeformed grid would be redundant.

A last note on frame of reference—this grid is an objective result calculated in a reference frame–free manner. However, any *verbal description* will not be reference-frame free, since our language does not allow us to describe relative position without one. Verbal description will involve some subjectivity, as many alternative descriptions are possible. Providing objective quantification of the differences observed in the total deformation is the role of the partial warp analysis that follows.

Neanderthal mean form. Figure 5 shows the grid for total deformation of the Norwegian mean form to the Neanderthal mean form. This grid illustrates several features considered typical of Neanderthals. The cranial vault is long and low, as expected, in association with reduction in the relative size of the parietal region (points 13, 14, and 15: notice the "pinching" evident in this area). The maxillary part of the face is relatively large, as seen in the overall expansion of the facial portion of the grid. This enlargement is especially marked in the vertical dimension: the rectangles in the maxillary region, below points 4 and 6 and above points 1 and 2, indicate greater increase in height than anteroposteriorly. The forehead is low, and the brow region is enlarged. The shift of the supraglabellar point (11) towards metopion (12) is involved with both of these changes. Enlargement of the brow region is additionally expressed in vertical expansion between points 10 and 11, and forward projection at 10. Point 9 (nasion) projects forward even more than point 10: notice the shape of the bulge in the grid anterior to this region, which juts farther in front of point 9 than it does in front of 10.

In some ways, however, this grid does not accord with the general view of a typical Neanderthal. The occipital region bulges only slightly, indicating that the occipital bun in the mean Neanderthal is little greater than that in the mean Norwegian. Some individual modern humans project much more markedly in this region (see examples in Yaroch, 1994a). Of course, the lack of information on the mediolateral dimension and more lateral landmarks on the bun prevent one from comparing other details of occipital bun morphology in this contrast.

While the face in the Neanderthal mean is relatively large overall, this is not true of all portions of the face. In particular, the orbit and anterior cheek region appear to be relatively small in size, despite the fact that Neanderthal orbits are uniformly described as large. In absolute dimensions they are indeed large, but these results indicate either that the orbit is not large relative to overall facial size, or that most of the orbital height is carried in the upper part of the orbit, not surveyed by my landmarks. Because I lacked landmarks to represent the upper part of the orbit, I collected traditional anthropometric data on orbital and dimensions and facial height from the literature to further investigate relative orbital size in Neanderthals.

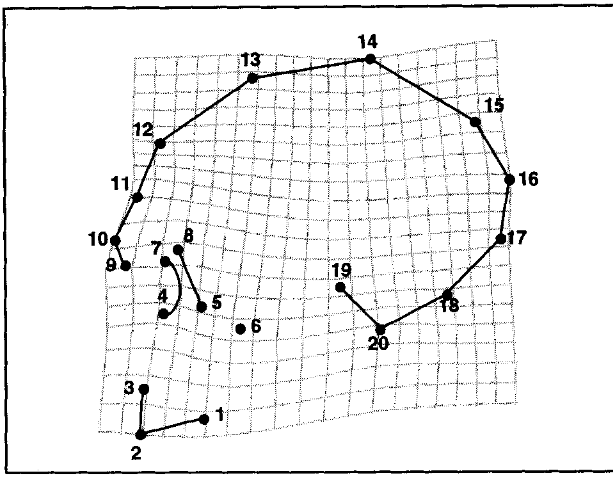

Fig. 5. Cartesian deformation of the Norwegian mean form to the Neanderthal mean form. If the grid in Figure 3A is deformed to match the landmark configuration in 3B, this deformed grid results. This illustration is much more informative about the shape differences between the two than is simple comparison of Figures 3A and 3B. The grid represents the total deformation, or total shape difference in this comparison, prior to breaking the shape difference down into components. This grid in an objective result, generated in a reference frame–free manner using the thin-plate spline; however, any verbal description of the grid will involve some subjectivity, and will incorporate some frame(s) of reference. In this comparison, the Neanderthal mean has a longer, lower braincase than the Norwegian mean, and the maxillary portion of the face is large, especially vertically. The forehead is lower, the brow is relatively large, nasion projects forward, and the orbit shifts upwards relative to other facial landmarks.

Table 1 shows data on orbital height, orbital breadth, and superior facial height (nasion-prosthion), as well as indices calculated by dividing orbital height and breadth by superior facial height. These values are shown for two modern groups, for the Neanderthal sample overall, for individuals Neanderthals, and for Kabwe and Petralona. I include data from the first 15 individuals with complete data from Gorný's (1957) Ugandan sample. I used Gorný's data to represent the range of these values within a modern human sample, because his is one of the only publications that includes measurements for individuals—usually only means are included. Data on mean values for Schreiner's (1939) Norwegians are also shown in Table 1. In Neanderthals, the ratio of orbital height to superior facial height ranges from .40 to .43, averaging .42. In the 15 Ugandans, the same index ranges from .39 to .55. The Ugandan mean value is the same as the Neanderthals', .42. No statistical comparison is made, since ratios cannot be treated statistically the way the original measurements might be (Atchley et al., 1976), but since the two samples have the same mean and the Neanderthal range fits easily within the Ugandan one, no statistical comparisons are necessary to state that the samples do not differ. The Norwegian mean value for this index is .47, indicating that the average male Norwegian has orbits a bit larger, relative to facial size, than the average Neanderthal. This agrees with what we see in the total deformation from Norwegian mean to Neanderthal mean. We have no way of knowing if this difference is statistically significant; however, it seems clear that Neanderthals do *not* have relatively large orbits. Instead they seem to have orbits proportioned appropriately for their large faces. Aiello and Wood (1994) have argued that orbit size is a good estimator of body weight in hominids. It seems likely that Neanderthal orbit size was in appropriate proportion to their body weight as well as their facial size. Petralona and Kabwe appear to have relative orbit sizes similar to Neanderthals and modern humans, consistent with

TABLE 1. Orbital height, orbital breadth, superior facial height, and indices comparing relative size of the orbit in Ugandans, Norwegians, Neanderthals, Petralona, and Kabwe

Group or specimen	Orbit width (mm)	Orbit height (mm)	Superior facial height (na-pros) (mm)	Orbit height/superior facial height	Orbit width/superior facial height
Ugandans (N = 15)					
Mean	42.8	33.5	79.2	.42	.54
Minimum	40.0	29.5	75.0	.39	.51
Maximum	45.0	38.0	83.0	.55	.57
Norwegians (N = 346 to 374)[1]					
Mean	41.0	33.7	72.0	.47	.57
Minimum			62.0	—	—
Maximum			87.0	—	—
Neanderthals	46.7	36.9	87.9	.42	.53
Minimum	43.0	36.0	85.0	.40	.49
Maximum	49.0	38.0	94.0	.43	.56
La Chapelle-aux-Saints	46.8	36.8	85.0	.43	.55
La Ferrassie 1	43.0	36.0	88.0	.41	.49
Guattari 1	49.0	37.0	(87.0)[2]	(.43)[2]	(.56)[2]
Shanidar 1	47.9	36.1	86.0	.42	.56
Shanidar 5	46.5	37.4	94.0	.40	.49
Amud 1	47.0	38.0	89.0	.43	.53
Petralona	48.0	37.0	89.0	.42	.54
Kabwe	51.03	39.0	95.0	.41	.54

[1]Depending on the measurement.
[2]Values in parentheses are estimated.

the results of Aiello and Wood. An index of orbital width divided by superior facial height, another indicator of relative orbit size, again shows that Neanderthals (minimum .49, maximum .56, mean .53) resemble modern humans (Ugandans: minimum .51, maximum .57, mean .54; Norwegians, mean = .57). Thus, taking absolute size into account in this very simple way shows that one characteristic attributed to Neanderthals is but one aspect of the more general characteristic "big." While the data in Table 1 are anthropometric data analyzed in a traditional way, it was the spline analysis that raised the correct question to ask.

Returning to the comparison in Figure 5, the orbit also appears to shift its position. The points defining the orbit, 4, 7, and 8, all move superiorly in this deformed grid, points 7 and 8 only slightly and point 4 to a more marked degree. Point 6 moves downward slightly relative to the orbital region and porion (19). This combination of upward movement at point 4 and a slight downward shift at point 6 produces a characteristic wave, or twist, in the deformation. I will henceforth refer to this feature of the deformation as the "orbitozygomatic twist." This twisting places the jugal point in a more inferior position relative to orbitale, so that it is on or below the Frankfurt Horizontal line. This unusual position of jugale has been previously observed in Neanderthals by Gorjanovič-Kramberger (1906), Boule (1921), and Patte (1955). The anterior zygomatic bone, as defined by points 4 and 5, does not increase in relative size with the maxillary and brow regions. The posterior portion of the zygomatic arch (between 6 and 19) increases slightly in both horizontal and vertical dimensions.

Nasion (9) is projected forward relative to the orbital region, in agreement with Coon's (1962) definition of midfacial prognathism—but the tooth row is *not* dragged forward with the nasal region, as Coon supposed. In descriptions of midfacial prognathism the teeth are supposed to be projected forward relative to the zygomatic region. (This is made explicit in Howells, 1989, and Trinkaus and Howells, 1979.) In this deformation, however, the lower maxilla (1, 2, and 3) projects very little relative to the anterior cheek region (points 4 and 5—notice that the line connecting landmarks 1 and 5 is almost vertical). Instead, the forward position of the face is associated with increase in the length of the temporal region, defined by points 6

and 19. In addition, the tooth row (represented by points 1 and 2) is shifted forward slightly simply because that part of the face is relatively large (as argued by Heim, 1976, and Smith and Paquette, 1989). While points 1 and 2 are somewhat farther forward relative to the anterior cheek, as anthropometric measurements have shown, this appears to be a consequence of these proportional differences rather than a shift localized to the nasal region and the tooth row. However, if a frame of reference at or posterior to porion is used, this difference in the temporal region and relative facial size may give a false impression of an anterior shift localized to the nasal region and the region of the tooth row—Neanderthal midfacial prognathism as it is classically described. See below, especially the discussion of La Chapelle-aux-Saints, for elaboration on this topic.

Kabwe and Petralona. Deformations of the Norwegian mean form to Petralona and Kabwe (Figs. 6A and 6B) are similar in showing relative reduction of the braincase especially superiorly, including the part of the frontal between metopion (12) and bregma (13), the entire parietal region (13, 14, and 15), and to a lesser extent the occipital plane (15, 16, and 17). They also show great heightening and deepening of the maxilla (between 4 and 1–3) and deepening of the anterior zygomatic arch (between 4, 5, and 6). They differ in frontal shape. The lower part of the frontal squama (11 and 12) increases in height in Petralona but not Kabwe. In Petralona the nuchal plane (17 and 18) is reduced proportionately with the rest of the neurocranium, while in Kabwe this region becomes relatively larger. Deformation in the brow region (9, 10, and 11) is similar in the two, with additional vertical increase in Kabwe. Kabwe shows more projection at nasion (9) than does Petralona: in Kabwe, the edge of the grid in front of point 9 bulges forward more than it does at point 10, as in the Neanderthal mean deformation. Petralona projects less in this area. In the maxilla, a clear shift in clival angle (points 2 and 3) in Petralona contrasts with little change in Kabwe.

Change in the orbital region in Petralona resembles the Neanderthal mean but appears more pronounced: the orbit appears shortened and is raised more dramatically. (The orbit in Petralona is actually about the size one would expect for his face; see Table 1). Kabwe has little or no vertical orbital reduction: although the point at the base of the orbit moves up relative to nasion and glabella, the zygomaticofrontal suture moves upwards also, so that the orbit does not appear to shorten. As we know that relative orbit size is similar in the Neanderthal, Petralona, and Kabwe, something is happening in the Neanderthal mean and in Petralona to make the orbit appear shorter in the deformation. This may be related to the orbitozygomatic twist, which is even more marked in Petralona than in the Neanderthals, but is absent in Kabwe. An analysis focused on this region, using landmarks (preferably in 3D), will be necessary to answer this question.

Comparing Figure 5 with Figures 6A and 6B, three observations are striking. First, it takes more warping of the Norwegian mean to generate Kabwe or Petralona than to produce the Neanderthal mean. Conversely, it ought to be easier to evolve a Norwegian from a Neanderthal than from either of the earlier forms. This is inconsistent with statements that modern humans are more closely related to these specimens than they are to Neanderthals (e.g., Rak, 1986; Howells, 1993). In the light of these grids, it is also difficult to argue that Kabwe and Petralona share a common, primitive facial position with modern *Homo sapiens*, as some authors have argued (e.g., Rak, 1986; Spencer and Demes, 1993). Second, the orbitozygomatic twist and the (false) impression of orbital shortening are even more strongly expressed in Petralona than in the Neanderthal mean. Third, it is Kabwe, rather than Petralona, that shows a similar degree of projection at nasion to the Neanderthal mean; and the orientation of the vertical lines between points 1 and 5 is almost as vertical in Kabwe as in the Neanderthal mean, indicating little projection of the tooth row. Both Kabwe and Petralona have large faces that may create an impression of prognathism at the tooth row. Neither one, however, shows the anteroposterior stretching in the temporal region that magnifies the impression of prognathism in the Neanderthal mean.

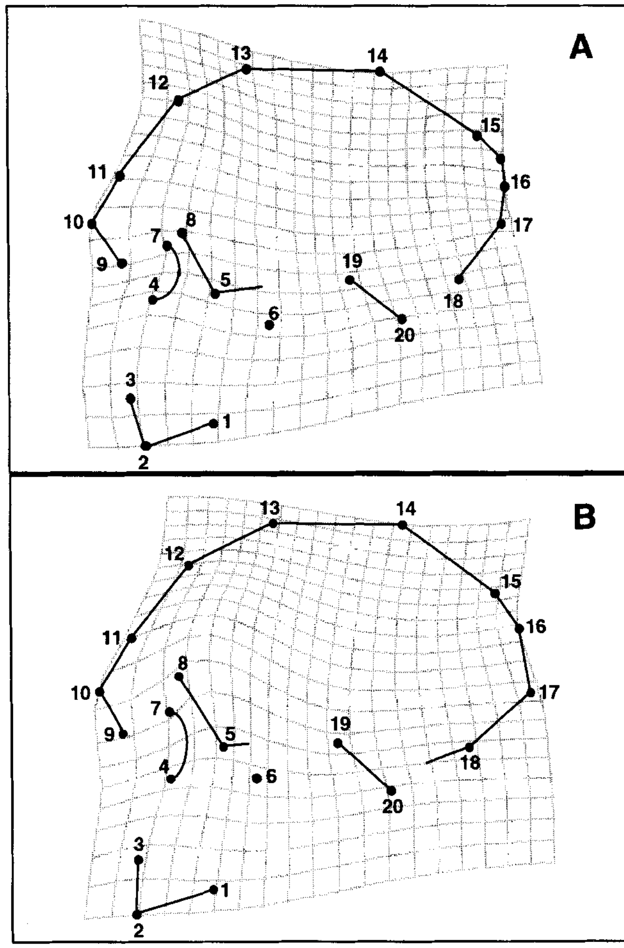

Fig. 6. Deformation of Norwegian mean (**A**) to Petralona's configuration, and (**B**) to Kabwe's configuration. Each grid represents the total deformation in that comparison, prior to breaking the shape difference down into components. These grids are much more deformed than the grid in Figure 3. Both show reduction of the braincase, especially superiorly, along with relative expansion of the brow region, great heightening and deepening of the maxilla, and deepening of the zygomatic arch.

Summary. These results confirm that, compared to the Norwegian mean, the Neanderthal mean has a long, low head, a low forehead, large brow ridges, and a large maxillary region. However, the occipital region projects only slightly relative to the Norwegian mean configuration, and less than in some modern individuals. The orbitozygomatic region also differs from classic descriptions. The orbit is not relatively large in Neanderthals. The anterior zygomatic region is relatively small in size in the Neanderthal mean, and the orbit shifts to a more superior position relative to other landmarks in the Neanderthal mean and in Petralona. The orbitozygomatic twist has been previously observed in Neanderthals, although characterized differently, as a low position for the jugal point (below the Frankfurt Horizontal); however, I have come across no mention of its presence in Petralona. As for prognathism, the relatively anterior position of nasion in Neanderthals is confirmed, but, contrary to Coon's (1962) and Howells' (1989) expectations, forward shift of the tooth row relative to the cheek region, associated with the projection of nasion, is absent. These results are consistent with Heim's (1976) and

Smith and Paquette's (1989) characterization of Neanderthal midfacial prognathism as a byproduct of the down and forward growth of a large face. Another contributor to the impression of prognathism involves the temporal region. In the Neanderthal mean, anterposterior stretching of the temporal portion of the zygomatic arch results in the tooth row being more forwardly placed relative to landmarks posterior to this region.

Kabwe and Petralona do not appear to be more modern than the Neanderthals, nor is there evidence that they share primitive shape features with modern humans. They share several primitive features with the Neanderthals, such as large maxillae, large brow ridges, and upwardly shifted orbits. Petralona also shares the orbitozygomatic twist. The frontal region in Petralona and Kabwe is shaped differently than in the Neanderthal mean: instead of having a low forehead like the Neanderthal, the neurocranium is reduced all across the top of the skull. In both Kabwe and the Neanderthal mean nasion is projected forward relative to the orbital region. Inasmuch as nasal forwardness measures midfacial prognathism, Kabwe is at least as prognathic as the Neanderthal mean.

Decomposition by partial warps

The previous discussion of total deformation consists of subjective descriptions of an objective result (the deformation grid) rather than canonical lists of features. Alternatively, the language of the partial warps provides a set of descriptors that are guaranteed to be geometrically independent and statistically complete, so that one can carry out statistical analysis as well as qualitative description. For each deformation of the Norwegian mean to a second form, the shape change was broken down into separate components. Inclusion of 20 landmarks allowed decomposition of the shape difference into 18 features, the uniform factor and 17 partial warps. Yaroch (1994a) includes a detailed description of all 17 principal warps, as well as statistics on uniform change and all 17 partial warps in the groups under study. Here, only the partial warps that show interesting contrasts between modern and fossil groups are discussed.

The Neanderthals differ significantly from more modern humans in only four of the 18 shape features. First, the Neanderthals differ in the largest-scale non-uniform feature, Partial Warp 1. Principal Warp 1, the *potential* for change at this scale, may be characterized as a shift of one diagonal of the skull, from the anterior alveolar area to the posterior parietal, relative to a diagonal extending from the lower frontal to the nuchal/mastoid region. This warp is analogous to the square-to-kite transformation discussed above (Methods; Figure 2B). Figure 7 shows a scatter plot for Partial Warp 1. In all the scatter plots herein, the origin represents the Norwegian mean form, and the scatter of points represents the magnitude and direction of the vector of displacement for that warp for each mean form or individual. For Partial Warp 1, a positive-x/positive-y displacement from the Norwegian mean characterizes the Neanderthal mean form, with further displacement in the y-direction in Petralona and Kabwe. The Neanderthal and Norwegian means are significantly different ($P < .001$), although the observed ranges of the Neanderthal and modern samples overlap. Four of the Neanderthals are either on the border of the modern range or within the modern range, and only one good specimen is distant from the modern mean (La Ferrassie 1). In contrast, Boule's reconstruction of La Chapelle, with a very high x-score, diverges from all the other hominids, whereas Heim's new reconstruction places La Chapelle with the other Neanderthals. Petralona and Kabwe have x-values similar to the Neanderthal mean, but their y-values exceed the observed ranges of both Neanderthals and moderns.

Figure 8A shows Partial Warp 1 for the Neanderthal mean form. In this change, the diagonal extending from the lower frontal to the mastoid region moves up and back relative to a diagonal from the posterior parietal to prosthion. This shift compresses the parietal area. At the same time, the maxilla increases in size and projects down and forward, increasing alveolar prognathism, the porion-mastoid-nuchal plane area moves up and back, and the lower part of the frontal

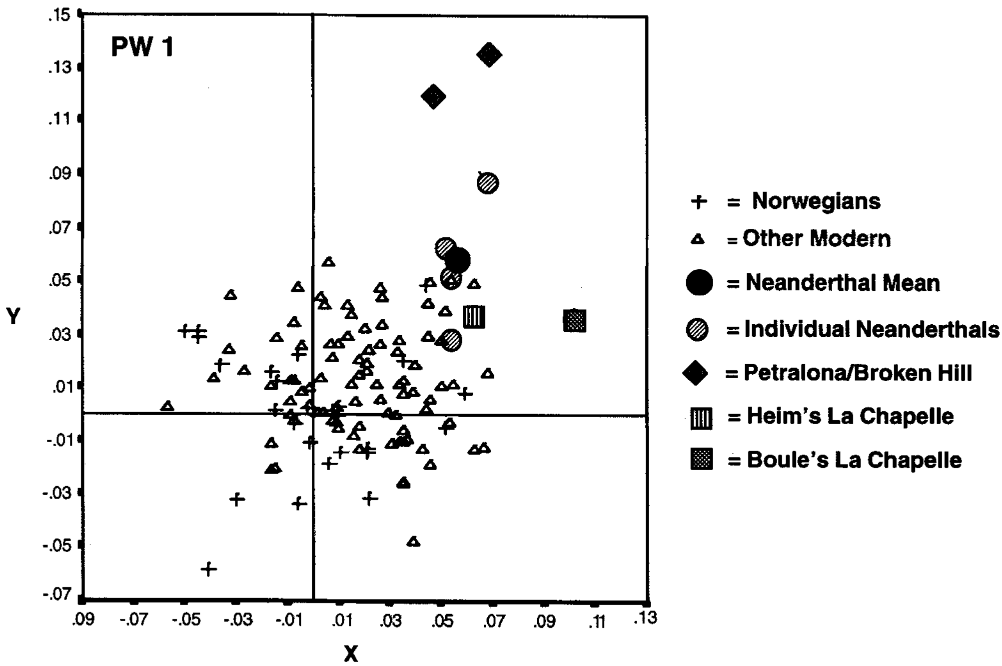

Fig. 7. Scatter plot of (x,y) scores for Partial Warp 1. The origin represents the Norwegian mean form, or starting form, and each point represents the magnitude and direction of the vector of displacement for Partial Warp 1 for that mean or individual. Norwegians are represented by triangles, other modern humans by plus signs, and Kabwe and Petralona by diamonds. Neanderthals are represented by circles: a closed circle for the Neanderthal mean, filled circles for individuals, except for La Chapelle-aux-Saints. Two reconstructions of La Chapelle-aux-Saints are represented, Boule's by a checkered square and the newer one by Heim by a striped square. In this shape feature the Neanderthals are intermediate between modern humans and the earlier specimens, with the exception of Boule's reconstruction of La Chapelle-aux-Saints, which is different from all the others. Heim's new reconstruction of La Chapelle-aux-Saints, however, places it with the other Neanderthals.

increases in height. This warp accounts for most of the increase in relative facial size in the Neanderthal mean, as well as much of the parietal reduction. Partial Warp 1 for the Kabwe-Petralona mean is shown in Figure 8B. (Since deformations for Kabwe and Petralona are very similar for this warp—note their proximity on the scatter plot—only one grid is shown). This grid resembles Partial Warp 1 for the Neanderthal mean, but has a higher y-score and thus involves additional deepening in the facial region, and greater vertical compression of the posterior portion of the braincase.

Neanderthals also differ from modern humans in Partial Warp 2, the second-to-largest-scale non-uniform feature. The second principal warp is characterized by movement of the most anterior and posterior points in one direction, while the central portion of the skull moves in opposition, producing bending of the skull about the middle. Figure 9 shows the scatter plot of (x,y) scores for Partial Warp 2. The Neanderthal mean form has a low y-value but an x-value nearer zero. The Neanderthal and modern ranges overlap, but the means are significantly different ($P = .001$). Two Neanderthals (Shanidar 1 and, barely, La Ferrassie 1) are within the modern human range, and the Neanderthal mean is on the border of the modern range, whereas Amud 1, Guattari 1, and Heim's reconstruction of La Chapelle are low on the plot. Boule's reconstruction of La Chapelle has an anomalous low x-value which disappears with Heim's new recon-

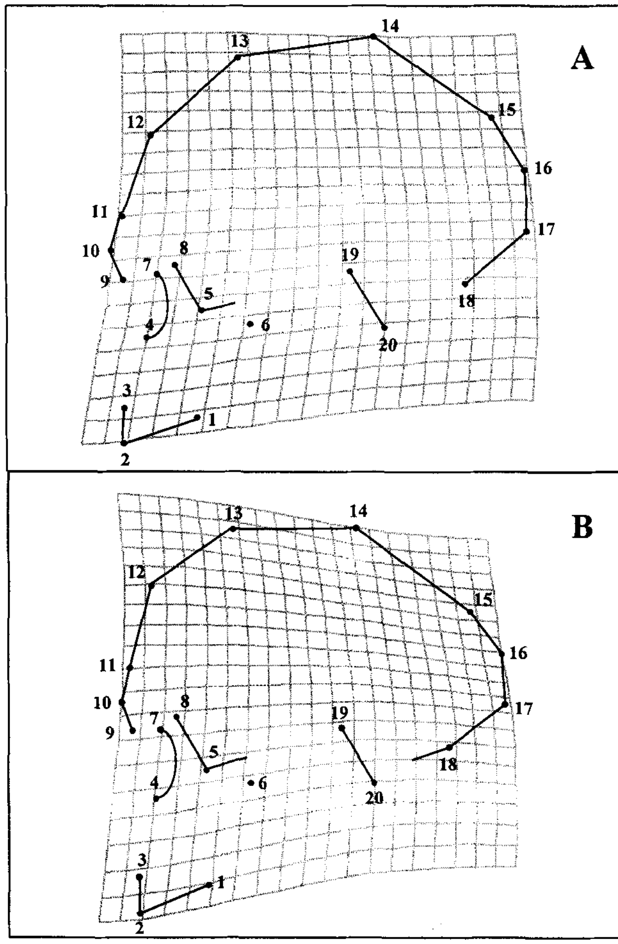

Fig. 8. Partial Warp 1 for (A) the Neanderthal mean form and (B) Petralona and Kabwe. These grids illustrate the shape difference at this scale when each is compared to the Norwegian mean. Shape change at this scale is similar to the square-to-kite transformation illustrated in Figure 2B. The deformation in this grid may be described as follows: a diagonal extending from the lower frontal to the mastoid region has moved up and back relative to a diagonal from the posterior parietal to prosthion. This shift compresses the parietal area, and the maxilla expands down and forward. The vertical component is more exaggerated in B.

struction. Petralona and Kabwe have y-values similar to the Neanderthal mean form, but relatively high x-values.

Figure 10A shows Partial Warp 2 with a negative y-score, an exaggerated version of the change characterizing the Neanderthal mean. The face and posterior neurocranium are bent upwards relative to the middle portion. This flattens the anterior part of the braincase that was not reduced by Warp 1, so that Partial Warps 1 and 2 combine to produce the longer, lower Neanderthal braincase. The more posterior facial points are pushed to a lower position relative to the anterior face, and porion is relatively lower than in the Norwegian mean. If Partial Warp 2 scores for Kabwe and Petralona are averaged (Fig. 10B), this warp involves slight lifting of the face and posterior neurocranium relative to the middle, as in the Neanderthal mean, corresponding to the negative value of the y-score. In contrast to the Nean-

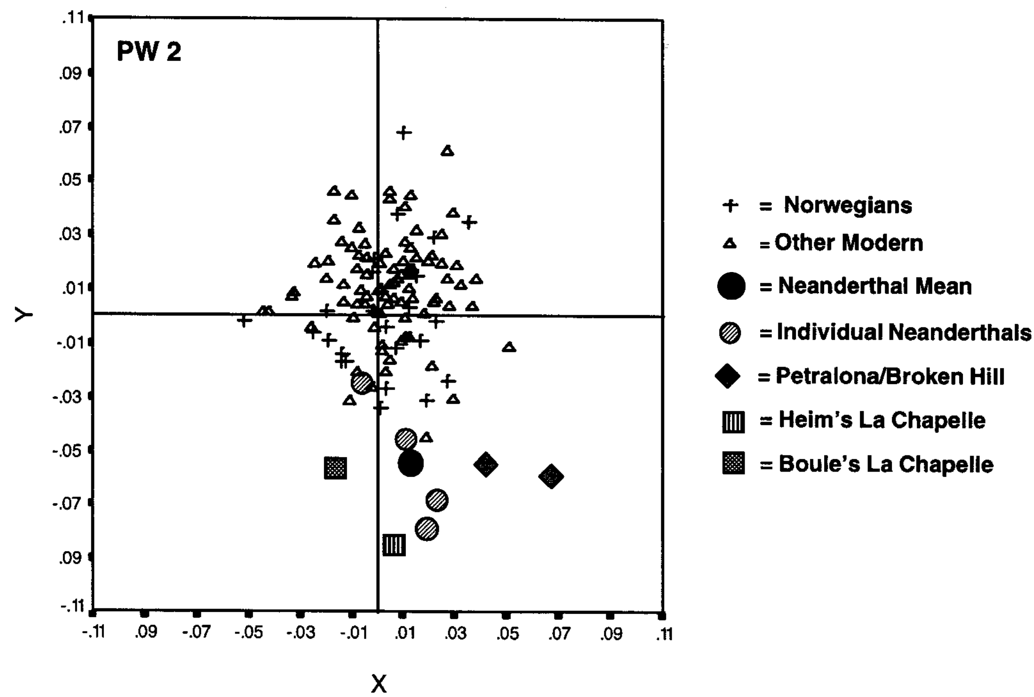

Fig. 9. Scatter plot of (x,y) scores for Partial Warp 2. The origin represents the Norwegian mean form, and each point represents the magnitude and direction of the vector of displacement for Partial Warp 2 for that mean or individual. All symbols are as in Figure 7. For this shape feature, modern humans, Neanderthals, and earlier *Homo* show three different states. Boule's reconstruction of La Chapelle has an anomalously low x-value that disappears in Heim's reconstruction.

derthal mean with its low x-score, the positive x-score in Petralona and Kabwe is associated with an anteroposterior increase in size of the front part of the skull (anterior to points 6 and 13) relative to the back of the skull (posterior to 14 and 19). In Petralona this latter deformation is a little more pronounced than in Figure 10B, and in Kabwe it is a little less pronounced (notice that on the scatter plot they have similar y-values but differ in their x-values).

Two localized facial warps also distinguish Neanderthals from Norwegians. The first of these is Partial Warp 13. Principal Warp 13 contrasts landmarks in the orbitozygomatic region and brow area with nasion (9), metopion (12), and the base of the temporozygomatic suture (6). Figure 11 shows the scatter plot for Partial Warp 13. The observed ranges of the Neanderthals and more modern humans overlap, but their means differ significantly ($P < .001$). For this warp, both reconstructions of La Chapelle are between the Neanderthal mean and the Norwegian mean. Kabwe is near the Neanderthal mean, but more distant from the origin. Petralona combines a low y-value with an x-value near zero.

Partial Warp 13 for the Neanderthal mean is shown in Figure 12. The brow ridge (9, 10, and 11) increases in size, with nasion (9) displacing forward more than glabella (10). The lower frontal (11 and 12) reduces vertically as the supraglabellar point (12) moves up and back and metopion (13) moves down and forward. The zygomaticofrontal suture (7 and 8) and orbitale (4) shift upward relative to the surrounding points, moving the orbit to a more superior position, and the base of the temporozygomatic suture (6) moves down and forward slightly. Partial Warp 13 for Kabwe is very similar but the deformation is more pronounced. Thus this warp accounts in part for the high position

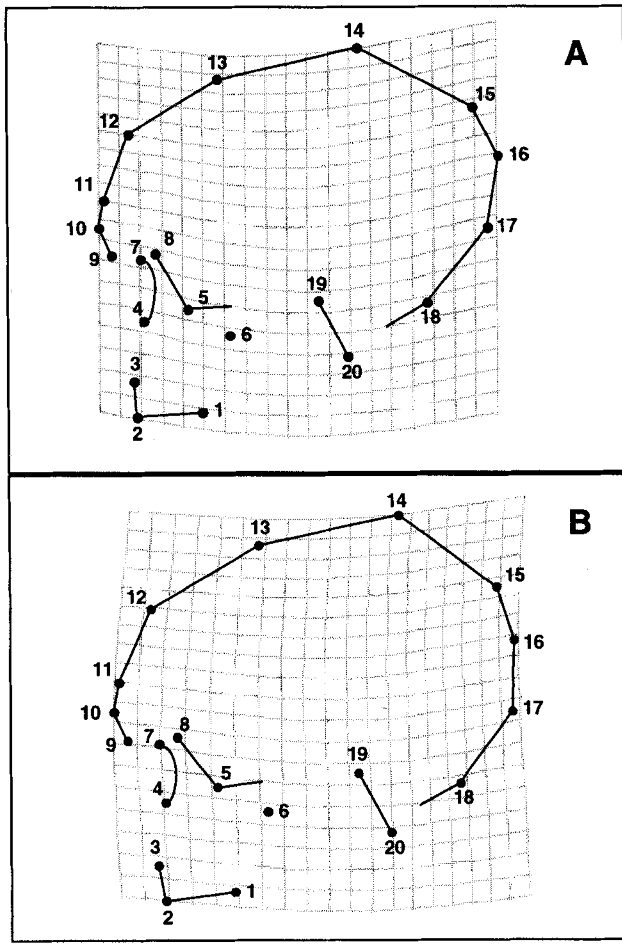

Fig. 10. Partial Warp 2. **A:** This grid illustrates Partial Warp 2 with a negative y-score, an exaggerated version of this warp for the Neanderthal mean. This grid shows bending of the skull across the middle, with the anterior and posterior portions moving upward. **B:** Partial Warp 2, averaged (x,y) scores for Petralona and Kabwe. This grid shows the bending of A, with the addition of relative expansion of the anterior part of the skull and the expanse of the posterior portion.

of the orbit, found in the Neanderthal mean, Petralona, and Kabwe, but it does not account for the twist in the orbitozygomatic region characteristic of Petralona and the Neanderthal mean. More importantly, this warp quantifies the forwardness at nasion observed in the total deformations of the Neanderthal mean (Fig. 5) and Kabwe (Fig. 6B), along with increase in height and projection of the brow, and lowering of the forehead. This warp shows a coordinated shift in what I have been referring to as three separate features (see section on Total Deformation). While the warp analysis does not demonstrate that brow projection, forehead height, and nasal projection represent a single trait in the evolutionary sense, it indicates that this is a useful working hypothesis. This is consistent with the view that large supraorbital size and low forehead are aspects of one feature (see, for example, Hylander et al., 1991, and Ravosa, 1991). Of the four warps that describe Neanderthals, this is the only one that shows any relationship to "midfacial prognathism" (other than the increase in relative facial size associated

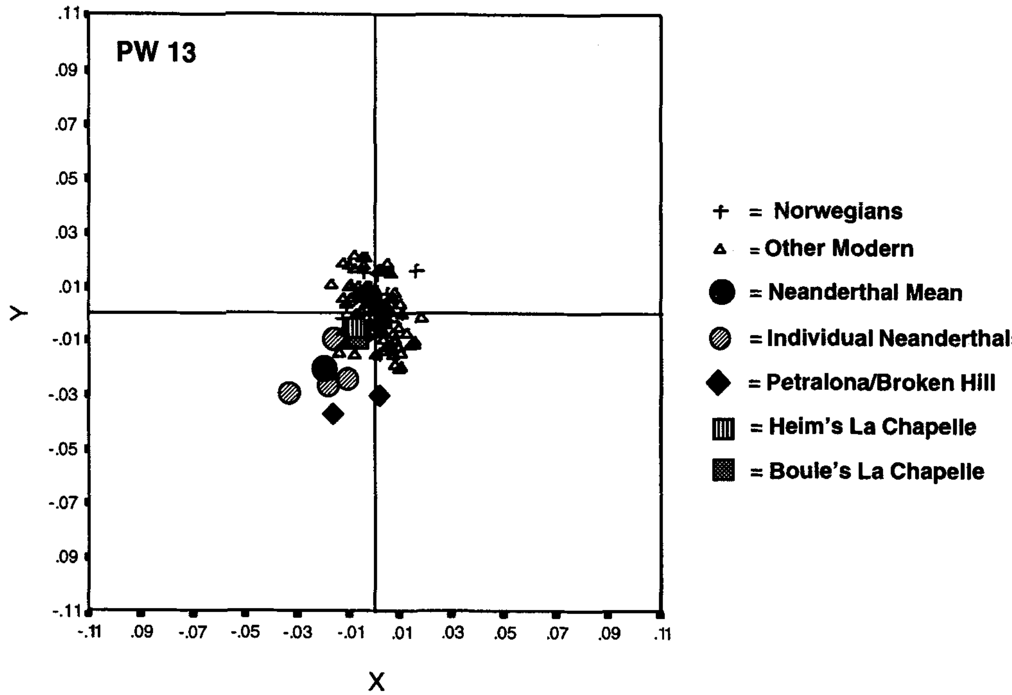

Fig. 11. Scatter plot of (x,y) scores for Partial Warp 13. The origin represents the Norwegian mean form, and each point represents the magnitude and direction of the vector of displacement for Partial Warp 13 for that mean or individual. Symbols are as in Figure 7. The Neanderthals differ from the Norwegians in this trait, with Kabwe scoring near the Neanderthal mean.

with Partial Warp 1). It is noteworthy that the maxilla is little affected by Partial Warp 13, and no (x,y) score for this warp has the potential to make the tooth row project relative to the anterior cheek region (Yaroch, 1994a; see Figs. 4.73 and 4.74). Thus the quantitative analysis confirms the impression gained from study of total deformation, that Kabwe is as midfacially "prognathic" as the Neanderthal mean.

Neanderthals also differ from more modern humans in Partial Warp 15, which involves predominantly the maxilla and the inferior portion of the orbit. As a principal warp, this feature contrasts prosthion (2), orbitale (4), and the base of the temporozygomatic suture (6) with nasospinale (3) and jugale (5). Figure 13 shows the scatter plot of (x,y) scores for Partial Warp 15. As a sample the Neanderthals are distinct from the Norwegians, with lower (x,y) values ($P <$ .003). Petralona's score for this warp is near the Neanderthal mean, while Kabwe is within the modern observed range. Figure 14 shows Partial Warp 15 for the Neanderthal mean form. While statistically significant, the difference between the Norwegian and Neanderthal means in this trait is very slight, and is barely detectable on the deformed grid. Very close inspection (of the grid and of principal and partial warp values) reveals the following changes: points 2 and 4 move up and back and points 3 and 5 down and forward, so that the maxilla expands slightly between orbitale (4) and nasospinale (2) and the nasoalveolar clivus become more vertical. Jugale (5) moves to a lower position relative to the Frankfurt Horizontal, and the orbit shortens a little as orbitale (4) moves upward. Petralona's (x,y) score is very similar to the Neanderthal mean but somewhat more distant from the origin. This warp appears to quantify that portion of the orbitozygomatic twist that is coordinated with

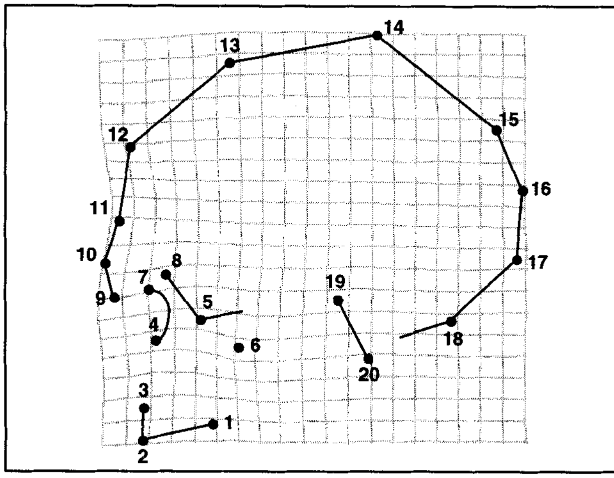

Fig. 12. Partial Warp 13 for the Neanderthal mean form. The brow ridge (9-10-11) becomes relatively larger, the forehead (11-12) relatively lower, and the anterior cheek (5) and orbit (4-7-8) shift upwards. Partial Warp 13 for Kabwe is similar but slightly more exaggerated.

change in clival angle. Petralona's high (x,y) score corresponds with the marked orbitozygomatic twist it shares with the Neanderthal mean. Some of the Neanderthals have a slightly more vertical clivus than the Norwegian mean—this feature, expressed much more strongly in Petralona, is quantified at least partly by this warp. Much of the shift in point 5 relative to nearby landmarks, found in the Neanderthal mean and in Petralona, is not represented by this warp, and it is likely that this warp is measuring more than one feature. Additional research at a finer scale, on landmark digitized from skulls or casts, could clarify this issue.

Three other warps of interest are Partial Warps 6, 8, and 16. For these features, Petralona and Kabwe are similar, and their partial warp scores are distinct from a state shared by Neanderthals and more modern humans. Figure 15 shows the scatter plot for Partial Warp 6. The Neanderthals do not differ significantly from modern humans in this feature. While they do, in fact differ significantly from the Norwegians in this trait ($P < .05$), the Neanderthals do not differ significantly from the Australians ($P = .086$), the Polynesians ($P = .142$), or the Ugandans ($P = .297$). The Neanderthal-Norwegian contrast appears to identify something unusual in the Norwegians rather than in the Neanderthals.

Figure 16 shows the scatter plot of (x,y) scores for Partial Warp 8, where a similar situation prevails: Kabwe and Petralona are paired at a distant position, while the Neanderthals show a modern state, despite the fact that they differ significantly from the Norwegians ($P = .001$). Again, the Norwegians, not the Neanderthals, are unusual in this feature. The other modern samples are more similar to the Neanderthals. The Ugandans and Australians also differ significantly from the Norwegians for Partial Warp 8 ($P < .001$ and $P < .01$ respectively), but none of the non-Norwegian modern samples are significantly different from the Neanderthals (Ugandans, $P = .06$; Australians, $P = .13$; Polynesians, $P = .23$, Eskimos, $P = .30$). For Partial Warp 16 (Fig. 17), Petralona and Kabwe are together, just outside the observed range for recent humans. The Neanderthals are not distinct from Norwegians or from the other modern humans in this feature.

Figures 18, 19, and 20 show Partial Warps 6, 8, and 16 for Petralona and Kabwe. This Partial Warp 6 (Fig. 18) involves increase in the size of the maxilla (points 1, 2, 3, and 4), especially anteroposteriorly, with coordi-

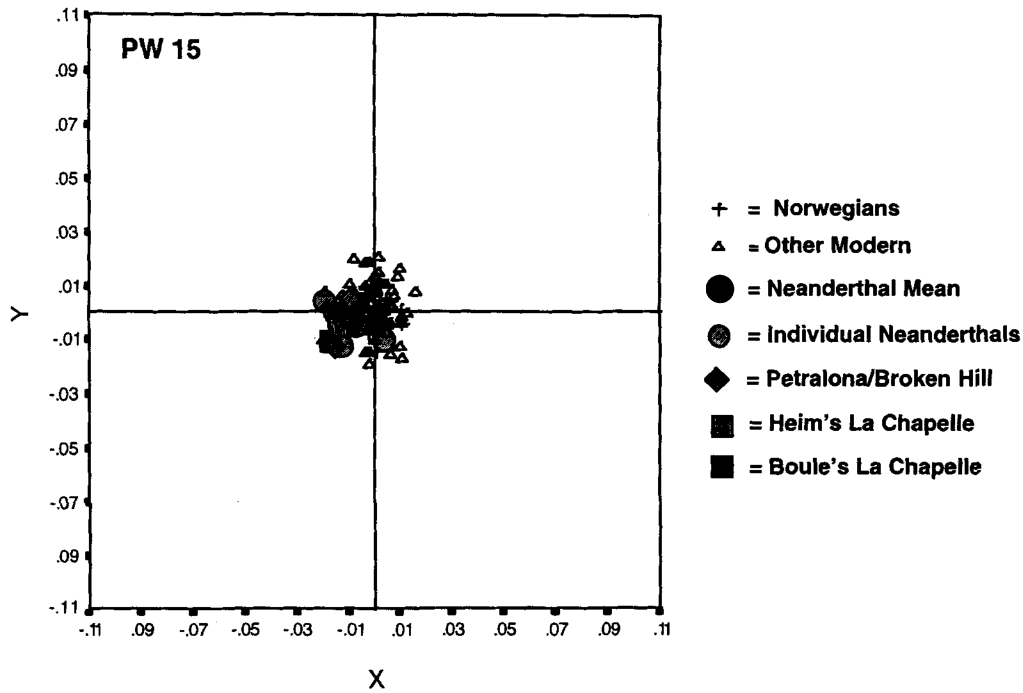

Fig. 13. Scatter plot of (x,y) scores for Partial Warp 15. The origin represents the Norwegian mean form, and each point represents the magnitude and direction of the vector of displacement for Partial Warp 15 for that mean or individual. Symbols are as in Figure 7. For this warp, the Neanderthals differ from the more modern samples, with Petralona sharing the Neanderthal state.

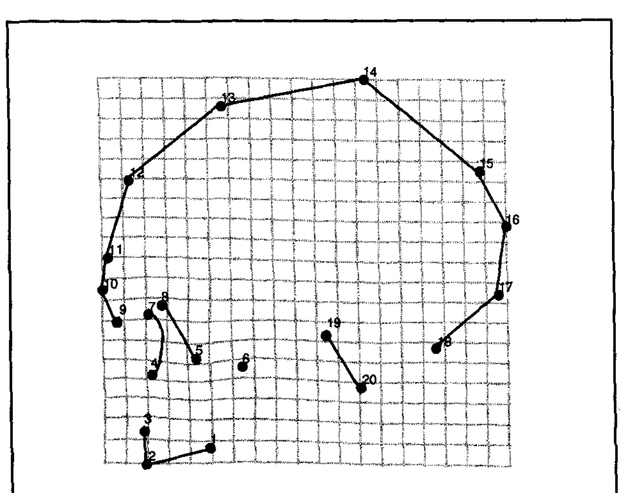

Fig. 14. Partial Warp 15 for the Neanderthal mean form. This change is very slight: jugale (5) moves upward relative to orbitale (4), and there is an extremely small change in the angulation of the nasoalveolar clivus (points 2 and 3). Partial Warp 15 for Petralona is very similar.

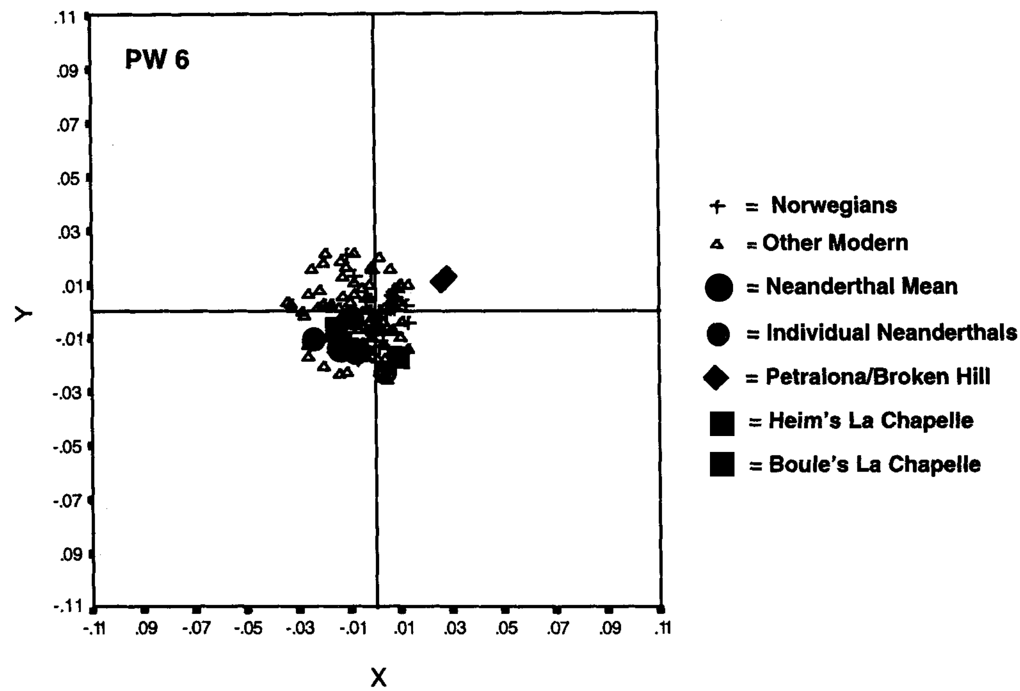

Fig. 15. Scatter plot of (x,y) scores for Partial Warp 6. The origin represents the Norwegian mean form, and each point represents the magnitude and direction of the vector of displacement for Partial Warp 6 for that mean or individual. For this warp, Petralona and Kabwe resemble one another and are separated from the modern humans and Neanderthals. The Neanderthals differ significantly from the Norwegians, but not from three of the four other modern groups, and thus are considered modern in this feature.

nated anteroposterior reduction of the temporal portion of the zygomatic arch (5 and 6). The frontal also reduces in relative size (11, 12, and 13). This warp accounts for some of the difference in facial proportion in Petralona/Kabwe compared to the Norwegian and Neanderthal means. They both have a reduced temporal region compared to the Norwegian and Neanderthal means, with a larger maxilla and a relatively smaller frontal. Partial Warp 8 (Fig. 17) for these two specimens is characterized by increase in relative size of the brow (9, 10, and 11), lower frontal (11 and 12), and parietal region (13, 14, and 15), associated with reduction in the upper frontal (12 and 13), the zygomatic bone (between 5 and 19), and the nuchal plane near inion (17). Thus, this warp accounts for some of the additional brow projection in these specimens, and quantifies some of the difference in nuchal plane shape. Partial Warp 16 (Fig. 20) expresses localized projection of the brow ridge (at 10), i.e., that projection that is not coordinated with change in other areas. Kabwe and Petralona show somewhat more of this localized projection than do the Norwegians and Neanderthals.

In summary, most of the shape contrasts between the Norwegian mean and the Neanderthal mean identified from the total deformation are quantified by the partial warp scores. For the Neanderthal mean, the two largest-scale warps transform the Norwegian mean into a longer, lower skull with a larger face. Partial Warp 13 is associated with increase in brow ridge size coordinated with reduction in forehead height, anterior projection of nasion relative to the zygomaticofrontal suture, and some upward shift in the orbit. Part of the orbito-zygomatic twist is quantified by Partial Warp 15.

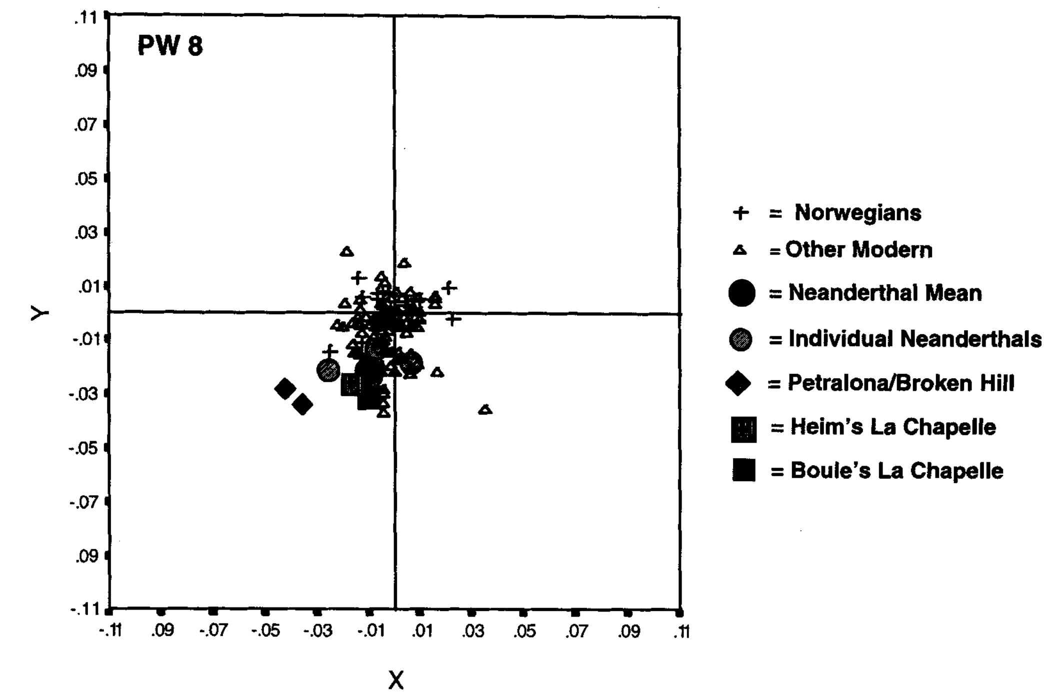

Fig. 16. Scatter plot of (x,y) scores for Partial Warp 8. The origin represents the Norwegian mean form, and each point represents the magnitude and direction of the vector of displacement for Partial Warp 8 for that mean or individual. Symbols are as in Figure 7. This scatter resembles the one in Figure 15 in that Petralona and Kabwe are similar to one another and distant from all the later hominids. The Neanderthals are significantly different from the Norwegians, but so are the Ugandans and the Australians significantly different from the Norwegian sample. The Neanderthals do not show significant difference from the other four modern groups, and thus are considered modern in this feature.

DISCUSSION

Application of the method of thin-plate splines has yielded a new and unique perspective on Neanderthal cranial shape. Results of this analysis confirm the presence of some of the characteristic Neanderthal features described in the literature, but indicate that other features have been mischaracterized. By and large, these mischaracterizations arise from limitations of traditional morphometric techniques, which until recently were the only methods of quantification available. A priori selection of anthropometric measurements generally means that only the features the researcher has already observed will be documented; important information may be left out. Traditional analyses may also suffer from neglecting to scale for overall size, from interpreting one aspect of a large-scale change as a localized feature, or from a misleading frame of reference.

The problem of scale may be illustrated with a simple example: orbit size. Characterization of Neanderthal facial morphology involves many repetitions of the word "large": large face, large nose, large supraorbital torus, etc. Neanderthal orbits have also consistently been described as large (e.g., Boule, 1911–1913; Sollas, 1924; MacCurdy, 1924; McCown and Keith, 1939; Heim, 1976). My results, in combination with anthropometric data from the literature, indicate that on the contrary, the average Neanderthal had orbits proportional to overall facial size (and perhaps to overall body size). While their orbits are indeed large in absolute dimensions, Neanderthal faces are large to match. Thus, it is helpful to recognize that Neander-

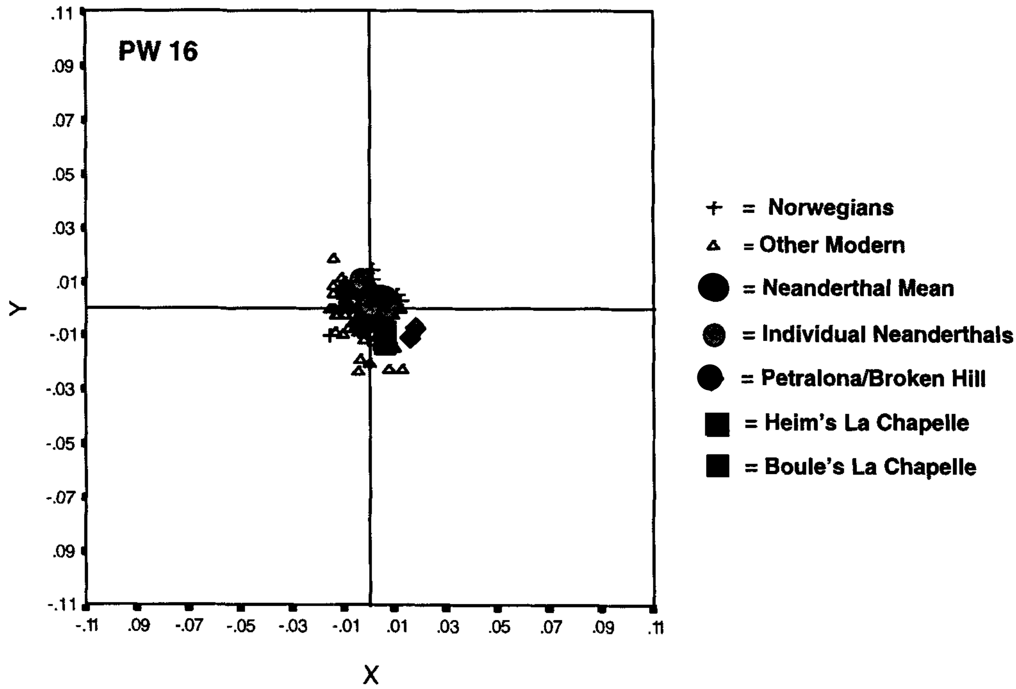

Fig. 17. Scatter plot of (x,y) scores for Partial Warp 16. The origin represents the Norwegian mean form, and each point represents the magnitude and direction of the vector of displacement for Partial Warp 16 for that mean or individual. This scatter shows a similar pattern to Figures 15 and 16, with Petralona and Kabwe very similar, but in this case the two earlier specimens are on the edge of the modern observed range, rather than distant from it. The Neanderthals share the modern state.

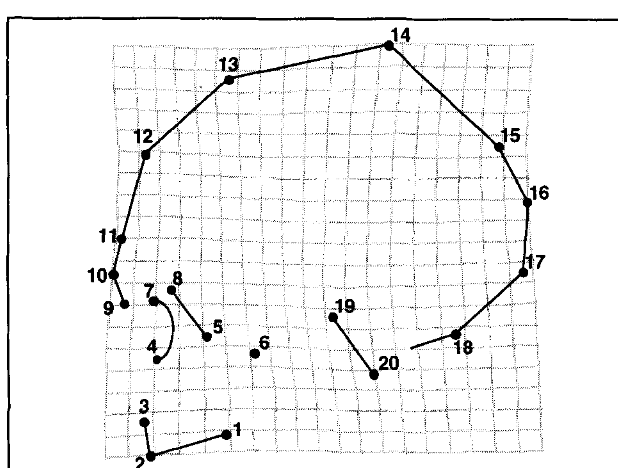

Fig. 18. Partial Warp 6 for Petralona and Kabwe: This warp involves increase in the size of the maxilla (1-2-3-4), especially anteroposteriorly, with coordinated anterposterior reduction of the temporal portion of the zygomatic arch (6-19), and reduction in relative frontal size (11-12-13).

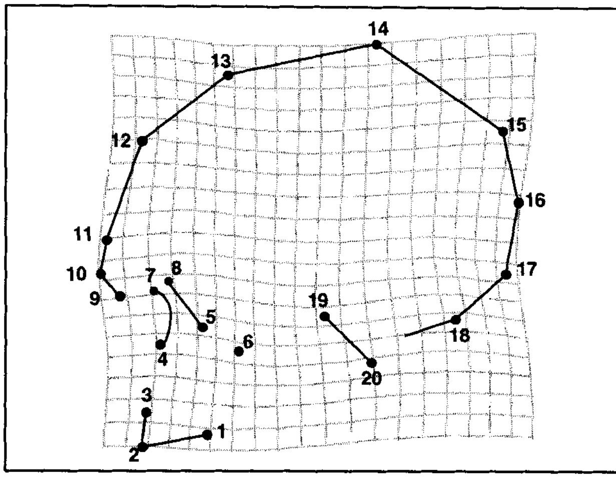

Fig. 19. Partial Warp 8 for Petralona and Kabwe: This Partial Warp 8 shows increase in relative size of the brow (9-10-11), the lower frontal (11-12) and the parietal region (13-14-15), associated with reduction the upper frontal (12-13), the zygomatic bone (5-6) and the nuchal plane (17-18) near inion (17).

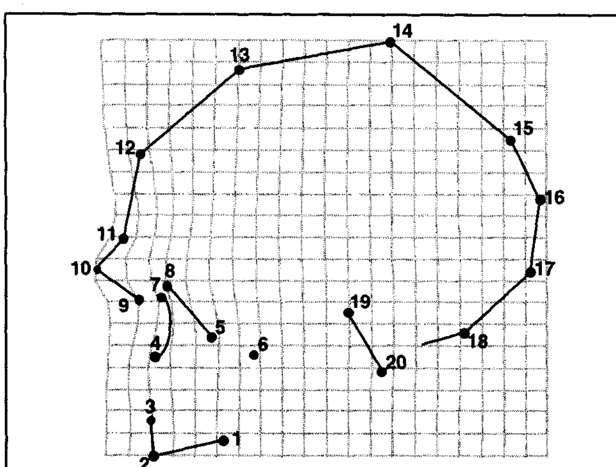

Fig. 20. Partial Warp 16 for Petralona and Kabwe: This warp quantifies localized projection of the brow ridge (9-10-11).

thals have large heads overall, to record this as one feature, and then to factor out absolute size before going on to make statements about the smaller subunits.

An example of a large-scale feature being confused with a localized one is the occipital bun. Convexity of the occipital plane has been used as a measure of occipital bun development (Hublin, 1988; Manzi, 1991). In fact, the Neanderthal mean form does *not* show marked convexity of the occipital plane compared to the Norwegian average, calling into question the idea of the bun as a "typical" Neanderthal trait. It is true, however, that two of the five *individual* Neanderthals studied have very marked occipital buns. La Chapelle-aux-Saints (both reconstructions) and Guattari 1 have impressive bulging of the oc-

cipital plane in their individual deformations (Yaroch, 1994a). This feature is not localized to the back of the skull, however. Partial Warp 12 (not discussed above, see Yaroch, 1994a) expresses *localized* bulging of the occipital plane. For this warp, all five Neanderthal individuals are well within the modern observed range. This implies that the large Neanderthal occipital bun, when observed, is not a trait in and of itself, but is instead an expression of a larger-scale feature: an overall longer, lower cranium. This conclusion is supported by the fact that the Neanderthals with the least occipital protrusion relative to the Norwegian mean, La Ferrassie 1 and Shanidar 1, also have an overall braincase form similar to the Norwegian mean (Yaroch, 1994a). Neanderthals do, in fact, show *some* localized occipital bulging: their mean for this trait is a bit higher than the Norwegian mean, although the difference is not significant. In fact, the Neanderthal mean value for localized occipital convexity is similar in degree to that of the Ugandan mean and to the mean of a French Mesolithic sample (Yaroch, 1994a). This result is in agreement Trinkaus and LeMay (1982) and Manzi (1991), who note that the occipital bun occurs to a greater or lesser degree in a number of modern groups.

A particularly tricky problem is that of frame of reference, one to which there was no good solution until quite recently. Results of this study show that the Frankfurt Horizontal, the most popular line/plane of reference in craniometric studies, is not necessarily an appropriate frame of reference for comparing Neanderthals, Petralona, or Kabwe to modern humans. This is because, when all landmarks are considered together, their orbits are shifted to a more superior position vis-à-vis other cranial landmarks, compared to modern humans. Consider, for example, the supposed high position of inion in Neanderthals (e.g., Sollas, 1908, 1924; McCown and Keith, 1939; LeGros Clark, 1978). In the Neanderthal mean deformation inion is not elevated, at least not in relation to other points on the braincase (see Fig. 5, landmark 17). The conflict is resolved when it is recalled that the position of inion was evaluated relative to the Frankfurt Horizontal. The superior position of orbitale in the Neanderthal mean skews the Frankfurt Horizontal so that inion will appear to be superiorly located even if there is no change in its position. The fact that the upward shift at orbitale is quantified by the localized facial warps 13 and 15 suggests that the "high" position of inion in Neanderthals reflects in large part a localized difference in facial shape.

Frame of reference also appears to be a problem with one of the Neanderthal "autapomorphies" suggested by Stringer et al. (1984): the superior position of the external auditory meatus. Evidently they refer to the feature noted by Martin (1926) and Patte (1955), and described by Trinkaus (1988) as positioning of the meatus "above the roof of the mandibular fossa, in the same horizontal plane as the zygomatic process of the temporal bone" (Trinkaus, 1988: 14). The external auditory meatus, as represented by its upper border at porion, is clearly not positioned higher in the Neanderthal mean form than in the Norwegian mean (point 19, Fig. 5). If there is any shift, porion is *lower* in the Neanderthal mean. It seems probable that this difference derives from positioning of the cheek region. In the Neanderthal mean the landmarks representing the zygomatic arch (and associated structures such as the mandibular fossa) are *lower* relative to porion and to the entire neurocranial contour, compared to the Norwegian mean. Future research may indicate that this feature is best described as a difference in facial shape, or as a change in relationship of the face to the neurocranium, rather than a difference in the position of the meatus itself.

The trait that has been plagued the most by problems with frame of reference is what has been termed "midfacial prognathism." Since Coon (1962) this trait usually has been described as conjoint forwardness of the nasal region and the tooth row, relative to more lateral facial structures. This study found that forwardness in the nasal region characterized the Neanderthal mean, but that the tooth row is *not* projected forward relative to the zygomatic bone. Therefore it is concluded that projection of the tooth row and the nasal region are two different features, a conclusion arrived at independently by Trinkaus et al. (n.d.). Projection of the nasal region is clearly present in the Neanderthal mean deformation, and is quantified by Partial

Warp 13. The same trait is pronounced in Kabwe's total deformation (Fig. 6B), and is confirmed by the proximity of this specimen to the Neanderthal mean for Partial Warp 13. Thus, this component of "midfacial prognathism" is as great in Kabwe as in the Neanderthal mean. In terms of the partial warp values, Kabwe is *more* prognathic than the Neanderthal mean.

Projection of the tooth row follows a different pattern. In neither the Neanderthal mean nor the Middle Pleistocene hominids does the tooth row project relative to the anterior cheek region, as it is supposed to do in the Neanderthals. Forwardness of the tooth row derives from two sources: first, overall large facial size (quantified by Partial Warp 1), and second, the anteroposterior "stretching" of the temporal area in Neanderthals (quantified by Partial Warps 1 and 13). Neither of these sources agrees with midfacial prognathism as classically described, where projection of the tooth row is evaluated relative to the zygomatic region. One might ask, then, why it has become a truism that midfacial prognathism, according to this description, is a "specialization" of Neanderthals found in no other hominids? As classically described, this prognathism is not present in the Neanderthal mean, and inasmuch as it *is* observed in the Neanderthal mean, it is shared with and exceeded by Kabwe!

Neanderthals were not always viewed as prognathic. Sollas (1908) noted that the Gibraltar cranium was very orthognathic "on whatever system we measure it." Soon after this, however, Boule (1911–1913) described La Chapelle-aux-Saints as *very* prognathic: "this snout-like arrangement, that I have already noted . . . is one of the most characteristic traits of our Mousterian. It contributes heavily to giving the face of this man a bestial aspect" (Boule 1921: 204, my translation). Henceforth, Sollas (1924) continued to point to variation in Neanderthals, with La Chapelle being prognathic and Gibraltar and the Krapina fragments being orthognathic; and Hrdlička (1930) described Neanderthal prognathism as "somewhat above average." However, the majority of researchers followed Boule in characterizing Neanderthals as prognathic in general (e.g. MacCurdy, 1924; McCown and Keith, 1939; Hooton, 1946). I have shown elsewhere (Yaroch, 1995, n.d.) that of the five Neanderthals I studied, only Boule's reconstruction of La Chapelle-aux-Saints shows midfacial prognathism as classically described: only in this individual does the tooth row project forward relative to the zygomatic region. Figure 21A shows total deformation of the Norwegian mean to Boule's reconstruction of La Chapelle. This deformation clearly shows the midfacial prognathism classically attributed to Neanderthals, with the tooth row projected forward relative to the cheek region—note the bending of the line between point 5 on the zygomatic and point 1 on the tooth row. This is what one would expect to find in the Neanderthal mean. Figure 21B shows total deformation of the Norwegian mean to Heim's reconstruction of La Chapelle-aux Saints. Here point 1 does *not* shift forward relative to point 5. Figure 22 shows the deformation of Boule's La Chapelle to Heim's La Chapelle. The tooth row very clearly withdraws relative to the cheek in the comparison. Probably not all the differences in this contrast are representative of differences in reconstruction. This grid also shows the kind of deformation one would expect if the photograph were an imperfect lateral view. Possibly the rear portion of the braincase was closer to the camera and the face farther away. Notice how the rear part of the braincase seems disproportionately large in this comparison, just as a person's foot in a snapshot may appear exaggeratedly large if it is too close to the camera. Examination of the original photograph also suggests this skull is not perfectly aligned, as do the partial warp data (this reconstruction shows an anomalous value on one of the large-scale warps not discussed herein). Because of this uncertainty these data were not included in calculation of the Neanderthal mean form. It is clear, however, distortion or no, that Heim's new reconstruction pulls the teeth beneath the cheek region to a very marked degree, so that La Chapelle now resembles the other Neanderthals in this trait. Heim's La Chapelle is also closer to the other Neanderthals in its partial warp scores (with the one exception mentioned above). Boule's La Chapelle differed markedly from all the

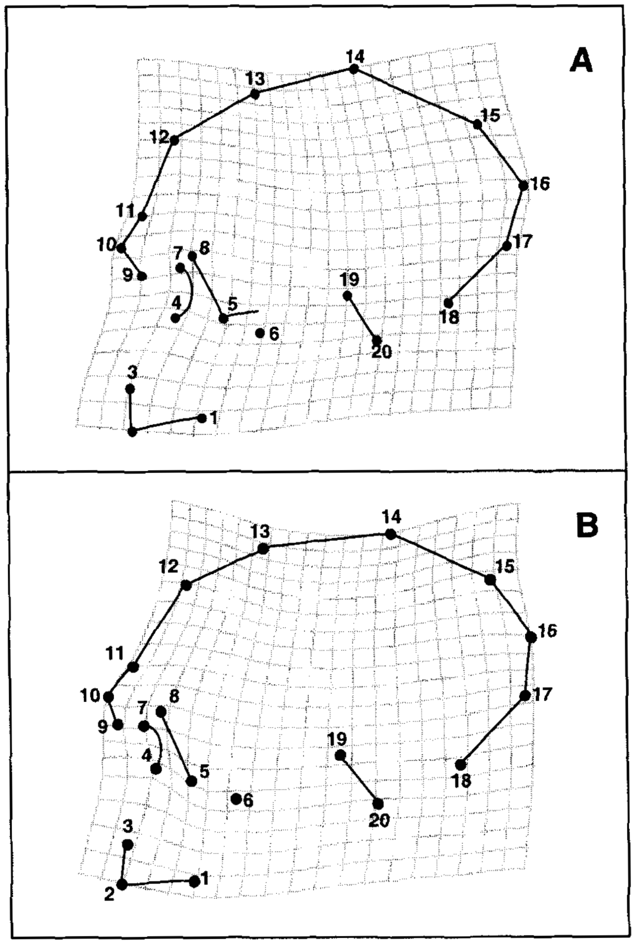

Fig. 21. Two different reconstructions of La Chapelle-aux-Saints. **A:** Deformation of the Norwegian mean to Boule's reconstruction of La Chapelle-aux-Saints. Notice the projection of the maxilla (1-2-3) relative to the cheek region (4-5-6). **B:** Deformation of the Norwegian mean to Heim's more recent reconstruction of La Chapelle. Notice that the maxilla does not project in the way it does in Boule's reconstruction.

hominids in the study for Partial Warp 1 (above) and also for Partial Warp 4 (not discussed here because the only noteworthy contrast was between La Chapelle and all other individuals; see Yaroch 1994a). Heim's La Chapelle has normal Neanderthal/hominid values for both of these warps.

It might be argued that Heim's reconstruction is simply one alternative, and not necessarily closer to reality than Boule's. Reading of Heim's (1989) account of the disassembly of Boule's reconstruction puts that notion to flight. For example, he notes that Boule's reconstruction produced a marked asymmetry in the cranial vault resulting from a forced contact between the anterosuperior part of the left parietal. This torsion pushed the left portion of the occipital forward relative to the right so that the two portions of the occipital were separated by a space about 1 cm—this gap was filled in with wax. In the face, errors were found in the reconstruction of the right orbit, the nasal cavity, and the palate. A fragment of the orbital floor was rotated 180 degrees so that what appeared to be the lacrimal canal was actually

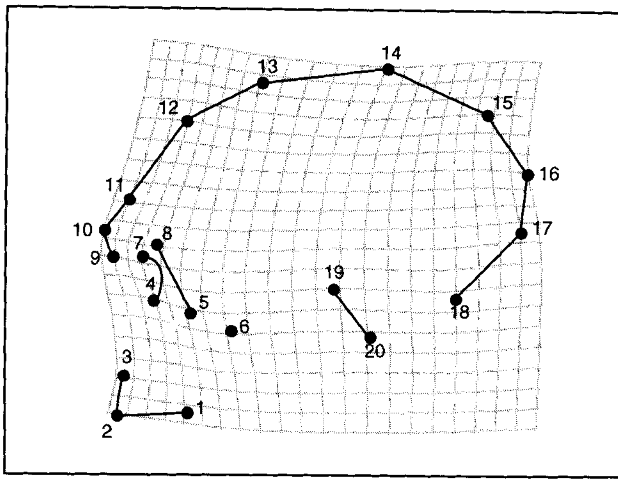

Fig. 22. Deformation of Boule's reconstruction of La Chapelle-aux-Saints to Heim's reconstruction of the same skull. Note that some of these differences may be linked to orientation of the skull in the photograph. However, it is clear that Heim's reconstruction pulls the maxilla back underneath the upper face.

the optic foramen. In order to hold this dubious arrangement together, a nail had been driven in on the internal surface of the ethmoid bone and surrounded with wax and plaster. Serious errors were also made in the reconstruction of the cranial base. In the light of these and other errors, there appears to be no question as to the superiority of Heim's reconstruction over Boule's. It is well known that Boule's reconstruction of the postcranial skeleton was erroneous (Manouvrier, 1888; Morton, 1926; Straus and Cave, 1957; Stewart, 1962; Trinkaus, 1985), and an effort has been made to correct the misapprehensions about Neanderthals that Boule's misreconstruction caused. However, despite the publication of Heim's new reconstruction, little effort has been made to correct the misunderstandings about Neanderthal head shape that are a consequence of Boule's work.

As long as the old reconstruction of La Chapelle is viewed as *the* "typical" Neanderthal, its kind of prognathism will be attributed to the group as a whole. Classic anthropometric measurements may confirm it in other Neanderthals: if projection of the tooth row is measured, say, relative to a biporionic line, the other Neanderthals will appear prognathic because 1) they have big faces (Heim, 1976), which grow down and forward (Smith and Paquette, 1989); and 2) they have anteroposteriorly expanded temporal regions as discussed above. Classical anthropometrics would not be likely to distinguish the general Neanderthal configuration from Coon's (1962) description of prognathism, except in the case where the researcher had already rejected Coon's description and chose measurements expressly to demonstrate this point.

Thus, results indicate that Neanderthals as a group can no longer be characterized as midfacially prognathic, even if some individuals not included in this analysis later prove to show the pattern characteristic of Boule's misreconstruction of La Chapelle. Projection in the nasal region is typical of (but not exclusive to) this group—but when one finds oneself using terms such as "prognathism at nasion," a terminological problem is clearly present. Since "prognathism" means forwardness of the jaw, it is not an appropriate term to use for the nasal region. "Prorhinism" would be a more apt description. According to this terminology, all five Neanderthals studied, as well as Kabwe, are prorhinic, and Boule's reconstruction of La Chapelle is both prorhinic and prognathic. This combination accounts for the *common*

use of the term "snout" in describing La Chapelle (e.g., Boule, 1921) and in Neanderthals in general (Rak, 1986), since a snout refers to projection of both nose and jaws. Now it appears that not even La Chapelle had a snout. Hence this term should be dropped from descriptions of Neanderthals as a group.

One feature La Chapelle *does* share with most of the Neanderthal sample is the moderately sized, upwardly shift orbit, with a twist in the zygomatic region pulling the jugal point below the Frankfurt Horizontal. This unusual position of jugale has been previously observed in Neanderthals by Gorjanovič-Kramberger, (1906), Boule (1921), and Patte (1955). Results of this analysis are consistent with this feature being a typical but not universal Neanderthal feature: Shanidar 1 expresses the twist only slightly, and has a jugal point above the Frankfurt Horizontal (Yaroch, 1994a). This feature is not unique to Neanderthals—it is expressed even more strongly in Petralona. I also found the orbitozygomatic twist in several early Upper Paleolithic European crania (Yaroch, 1994a), although the trait is absent in all the late European Upper Paleolithic crania I have been able to analyze. It is also very rare in recent humans: I found it in only two of 156 recent skulls. With these two exceptions, the orbitozygomatic twist has been observed only in prehistoric Europeans, and when this trait is better understood it may prove to be a European regional trait.

This study does not support characterization of Neanderthals as "specialized" or "autapomorphic." Both study of the total deformation and quantification by partial warp analysis return the same result: the Neanderthals overlap with more modern human in every feature identified, and also share important features with Petralona and Kabwe. Results of this study add classic Neanderthal midfacial prognathism to a growing list of traits that, once believed to be autapomorphic in Neanderthals, are now known to occur commonly in other human groups. For example, recent work by Franciscus and Trinkaus (1995) on the retromolar space in Neanderthals shows how uncritically one Neanderthal "autapomorphy" has been accepted. According to these authors, 75% of Neanderthal mandibles have this feature, as compared to 60% of a combined Skhul/Qafzeh sample, and 30% in the European Upper Paleolithic. Another suggested Neanderthal autapomorphy is the anterior mastoid tubercle (Hublin, 1988; Condemi, 1988), a feature present in 35% of European Neanderthals, two of five specimens in a combined Skhul/Qafzeh sample, and 20% of specimens from the early Upper Paleolithic of Europe (Frayer, 1992; this article discusses several other problematic Neanderthal "autapomorphies"). Some postcranial "peculiarities" of Neanderthals may not be unique. For example, morphology of the pubic ramus for pre-Neanderthal *Homo* is unknown (Kennedy, 1992), and the Neanderthal state is likely to be primitive (Rak, 1992). One must seriously question the truism that European and Near Eastern Neanderthals share a suite of derived features that distinguish them from other human groups. To be convincing, arguments for Neanderthal autapomorphy need to be accompanied by quantitative data both from several Neanderthals and from a variety of modern and fossil groups.

Obviously assessment of the evolutionary relationship of Neanderthals to other human groups should be based on all available data, including post-cranial morphology, nonmetric cranial characters, and aspects of cranial shape not represented in *norma lateralis*. In particular, this study examines Neanderthal cranial shape in two dimensions only. The mathematics of the thin-plate spline apply equally well to three dimensions, and such an approach offers great potential for further understanding of Neanderthal craniofacial shape. Other three-dimensional geometric approaches may also offer new insights. However, two-dimensional studies such as this one still have much to offer. In the case of Neanderthals, many, if not most, important Neanderthal cranial features are represented, at least approximately, in lateral view. Some features, in particular midfacial prognathism, are consistently characterized in terms of two or, more commonly, one dimension. These models can be tested effectively using 2D data. Studies that argue for a distant rela-

tionship between Neanderthals and modern humans tend to emphasize features expressed in the lateral view, whereas studies arguing that Neanderthals were ancestral to modern humans tend to emphasize the frontal view (Willermet, 1994). Thus it is likely that data from *norma frontalis* would find the Neanderthals even less distinct.

In any case, I am not aware of any published study that genuinely assesses Neanderthal cranial shape in three dimensions. Multivariate studies of traditional anthropometric measurements are not truly three-dimensional studies: they use landmarks from all three dimensions, but since they are not geometric, i.e., do not take into account the relationships among the landmarks, such analyses can only be regarded as studies of many two-dimensional measurements, which is not the same thing. The analysis here, while it assesses two dimensions only, quantifies the differences in those two dimensions exhaustively—*all* information in the landmarks is used.

Another potential problem with the approach taken in this study is the use of photographs and scale drawings as a source of data. Landmark data taken from photographs and scale drawings are inferior to those taken using a 3D digitizer on a cast or original specimen. Error may be introduced by photographic distortion or difficulty in identifying the landmarks on the image. Landmarks used in this study were shown to be accurately identifiable on photographs. Photographic distortion is a more serious problem, but in practice it is not as great a problem as might be anticipated. When significant distortion is present it is usually readily evident from the photograph itself, from its deformed grid, and from its partial warp data. Several photographs were discarded from the study because of distortion, as were many others because landmarks were not clearly pictured. Most importantly, the shape features identified on the total deformation and in the partial warp analysis are clearly present in casts of Neanderthal crania. A conclusion about shape that was an artifact of photographic distortion surely would be absent in the specimens themselves. It must be emphasized that any conclusions about shape differences reached in this kind of analysis *must* be referred back to the total deformation, to images from other views, and to casts of the fossils. There is no excuse (and, in my experience, no temptation) to disappear into a morphometric fairyland where photographic distortion is taken to represent biological difference.

The partial warp analysis could be made more complete by adding more landmarks. Recall that the number of warps generated is entirely dependent on the number of landmarks in the starting form. A dataset incorporating more landmarks would generate additional partial warps, yielding more detail about shape difference. In a similar study with more partial warps, one of the large-scale features from this study might produce a signal on several warps, at which point the researcher might try to evaluate whether more than one character was subsumed under that original large-scale warp. In fact, correlation and discriminant analysis indicate that partial warps 1 and 2 herein may represent a single feature (Yaroch, 1994a). (Partial warps 13 and 15 show no correlation with one another or with Partial Warps 1 and 2). In addition, an analysis of this same dataset that focused on the neurocranial outline, and included only 12 landmarks, generated a first partial warp that appeared to subsume both Partial Warps 1 and 2 (Yaroch, unpublished data). If Partial Warps 1 and 2 did indeed represent a single feature, it would indicate even fewer differences between Neanderthals and modern humans.

An approach incorporating more landmarks and generating more warps might also pick up on subtle differences this analysis was unable to identify. Error from using images rather than original specimens for landmark data might tend to obscure smaller shape differences between Neanderthals and recent humans. Future documentation of small differences of this kind may well serve to set Neanderthals apart from all other hominids as they classically have been. However, it is significant that several of the features heretofore considered quintessentially Neanderthal do not seem to be present in the Neanderthal skulls themselves, midfacial prognathism being the most striking example.

Despite the fact that this analysis does not completely represent every aspect of Neanderthal cranial shape, the results do justify some conclusions. One can directly evaluate some published characterizations, particularly those that are proposed in terms of one or two dimensions. Results of this study frankly disagree with the classic characterizations of midfacial prognathism (Coon, 1962; Trinkaus and Howells, 1979; Howells, 1989). These descriptions are articulated in terms of relative anteroposterior positions of landmarks and are readily testable in cranial data taken from a lateral view. The fact that Boule's erroneous reconstruction of La Chapelle-aux-Saints is the only "Neanderthal" to show this morphology is unlikely to be a coincidence. Our idea of typical Neanderthal form appears to be at least partly derived from "the Neanderthal that never was."

SUMMARY AND CONCLUSIONS

In this paper the method of thin-plate splines, a new geometric technique for illustrating and quantifying biological shape difference, is applied to the problem of characterizing Neanderthal cranial shape. The field of geometric morphometrics offers techniques that allow one to get very rich information on shape difference from landmark data. Geometric methods differ from more traditional morphometric approaches in that information about relationships among landmarks is preserved—the form one started with can be reconstructed from the data. One geometric approach, the thin-plate spline, allows the researcher 1) to illustrate shape difference as a D'Arcy Thompson–style deformed grid, and 2) to decompose the shape difference into series of components based on scale. These components, the partial warps, are geometrically independent (no shape information is counted twice) and are exhaustive (the partial warps sum to the total shape difference). This new technique is applied to an old problem, Neanderthal cranial shape, and offers new perspectives on what cranial features are typical of Neanderthals.

Thin-plate spline analysis confirms the presence of some proposed Neanderthal features, such as the long, low cranial vault and relatively large maxillary region. However, posterior protrusion of the occipital in Neanderthals is probably a consequence of large-scale shape difference related to a long, low vault. The Neanderthal low forehead and large brow ridges are probably expressions of a single feature. Projection of nasion anterior to the lateral orbital border is coordinated with these changes in brow and forehead morphology, but is not coordinated with change in the maxillary region (contra Coon, 1962). Thus the term "midfacial prognathism" as currently applied describes more than one feature: projection of the nasal region and projection of the tooth row relative to the cheek region. The latter is not found in the Neanderthal mean, nor in any of the good individual specimens. Only Boule's flawed reconstruction of La Chapelle-aux-Saints shows the type of midfacial prognathism commonly attributed to Neanderthals. This trait disappears in Heim's new reconstruction of La Chapelle. The term prorhinism is proposed to refer to nasal forwardness, as an alternative to calling it "prognathism," which it is not. Prorhinism is common in Neanderthals, but not unique to them: the Kabwe specimen is even more prorhinic than the Neanderthal mean form.

This analysis uncovered previously undescribed features in the orbitozygomatic region of the Neanderthal mean. First, the orbit is shifted superiorly relative to other cranial landmarks. This shift in orbit position accounts for the previously observed fact that jugale is located below the Frankfurt horizontal in Neanderthals. The positioning of the orbit in Neanderthals renders suspect features defined relative to the Frankfurt Horizontal. An example is the "high" position of inion in Neanderthal, which appears to be an artifact of the Neanderthals' superiorly positioned orbitale, which skews the Frankfurt Horizontal. The "high" position of the external auditory meatus also seems to be an artifact of frame of reference. It may be a byproduct of a difference in zygomatic morphology, and thus a facial rather than a neurocranial difference. Second, results indicate that Neanderthals do not have relatively large orbits. While Neanderthal orbits are large in absolute measurements, they appear to have orbits appropriately proportioned to their large faces. The

third unusual feature in this region is the orbitzoygomatic twist, a shift in the relative positions of landmarks in the lower orbital and zygomatic region which pulls the jugal point below the Frankfurt Horizontal. Precisely how this twist in the deformation grid is actually generated by the three-dimensional morphology of the region has yet to be explained. Of these three unusual orbitozygomatic features, both Kabwe and Petralona share the upward shift in orbital position with the Neanderthal mean, and have orbits comparable to the Neanderthals in relative size. Petralona also has a marked orbitozygomatic twist. Kabwe does not.

Inasmuch as Neanderthal cranial morphology is represented by these 20 landmarks in a lateral view, results of this analysis do not support interpretation of Neanderthal cranial shape as unique. In the analysis of partial warps Neanderthals do not differ from more modern humans in 14 of the 18 features defined. In the four partial warps where the Neanderthals differ, the observed ranges of the Neanderthal and more modern samples overlap. For Partial Warp 1, the Neanderthals are halfway in between more modern humans and Petralona/Kabwe (with the exception of Boule's La Chapelle-aux-Saints, see Yaroch, 1994a, 1995, n.d.). For Partial Warp 2 the Neanderthals are not intermediate. Instead, Neanderthals, Petralona/Kabwe, and post-Neanderthal humans show three different states for this feature, with the Neanderthals somewhat closer to the modern humans than are the earlier specimens. This feature comes closest to being a Neanderthal autapomorphy—but given the substantial overlap with modern humans and the fact that a Norwegian individual scores directly on the Neanderthal mean, the term autapomorphy seems inappropriate. In any case, Partial Warp 2 does *not* represent a trait where Neanderthals are distinct, with modern humans sharing a more primitive state with Petralona and Kabwe. For Partial Warps 13 and 15, the two facial warps where Neanderthals differ significantly from more modern humans, Kabwe shares the Neanderthal state for Warp 13, and Petralona shares the Neanderthal state for Warp 15.

For three warps, Petralona and Kabwe differ from all later human samples. For Partial Warps 6 and 8, warps involving primarily the face and posterior neurocranium, these two individuals are distinct from the later samples, both Neanderthal and post-Neanderthal. Partial Warp 16, localized projection of the brow ridge, shows a similar pattern but in this case Petralona and Kabwe are on the edge of the later human observed range. The Neanderthals show the modern state for these three warps. Of 18 features, *for none of them did Petralona and Kabwe share the more modern state with the Neanderthals having a different one.* Some authors argue that hominids such as Petralona and Kabwe have more in common with modern humans than either does with the Neanderthals (e.g., Howells, 1974; Rak, 1986, 1992; Santa Luca, 1978, 1980). Recently there have been suggestions (e.g., Stringer and Gamble, 1993; Howells, 1993) to assign the Neanderthals to a separate species, *Homo neanderthalensis,* but to retain Kabwe and Petralona in *Homo sapiens,* based on derived features in Neanderthals and primitive features shared by modern humans and Petralona/Kabwe. The results of this analysis do not support this classification. Instead, they add to the growing list of features that are not, after all, unique to Neanderthals. There is a tendency to overstate the case for Neanderthal autapomorphies; special care should be taken to examine variation in both the Neanderthals and other hominid groups before attributing unique features to the Neanderthals.

The conclusions reached here are consistent with what the eye can see when craniofacial profiles of living humans are compared with those of the available Neanderthal sample and the two earlier Petralona and Kabwe specimens. That is, less change is needed to produce a Norwegian out of a Neanderthal ancestor than out of what is represented by either of the earlier crania. Figure 23 shows transformation in the direction of evolutionary time, that is, from mean Neanderthal to mean Norwegian. To make the average Neanderthal into the average Norwegian, one need only reduce the relative size of the tooth-bearing portion of the skull and relative size of the brow region, and arch the braincase slightly, while maintaining the size of the orbit.

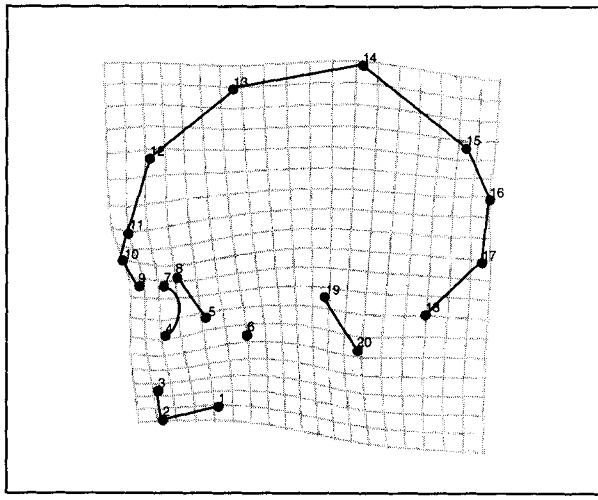

Fig. 23. Deformation in the direction of evolutionary time: Deformation of the Neanderthal mean to the Norwegian mean. The tooth row and brow regions shrink, and the braincase becomes more arched.

One important aspect of the method of thin-plate splines is that it has the potential to pick up on shape differences undreamed of by the researcher. Whereas in traditional anthropometrics the anthropologist chooses measurements to represent the features s/he believes to be important, geometric morphometrics involves choosing landmarks, not measurements. The thin-plate spline quantifies all the shape difference represented by those landmarks in a reference-frame free manner. It could be argued that choice of landmarks is as arbitrary as choice of measurements, but this is not true. In practice the tendency is to use as many landmarks as possible, given the limitations of the data; and to completely miss an important feature one must leave that region out entirely, not just neglect the critical measurements that might have defined that feature. In this analysis, all landmarks that could reliably be identified on the images and were preserved on a reasonable number of Neanderthal crania were included. The results were in several ways a surprise. In particular, the aberrant nature of Boule's La Chapelle and the absence of classic Neanderthal midfacial prognathism in the Neanderthal sample were completely unanticipated. It is likely that application of this technique to other anthropological problems would yield equally rewarding, and possibly equally startling, insights.

ACKNOWLEDGMENTS

This paper derives from my doctoral dissertation, and all the people I acknowledged in my dissertation I thank again here. In particular I thank the doctoral committee, Drs. C. Loring Brace, A. Roberto Frisancho, Frank B. Livingstone, and Fred L. Bookstein. Drs. Brace and Bookstein provided constructive criticism of this manuscript, as did Dr. Miriam Leah Zelditch. I also thank two anonymous reviewers for their helpful comments and suggestions. All errors are, of course, solely attributable to the author. Dr. James Rohlf wrote the program TPSpline that I used to analyze the data and to generate deformed grids for the illustrations. I owe special thanks to Dr. Erik Trinkaus, who contributed a photograph of the new reconstruction of the La Chapelle-aux-Saints cranium, which I would otherwise have been unable to include in the analysis. I am also grateful to Bennett Fauber of the University of Michigan Statistical Research Laboratory, for rescuing my dataset from a dire fate. Finally, I thank the Editor, Dr. A. Theodore Steegmann, for his patience and encouragement.

LITERATURE CITED

Ahlström T (1996) Sexual dimorphism in medieval human crania studied by three-dimensional thin-plate spline analysis. In LF Marcus, M Corti, A Loy, GJP Naylor, and DE Slice (eds.): Advances in Morphometrics. New York: Plenum, pp. 415–421.

Aiello LC, and Wood BA (1994) Cranial variables predict hominid body mass. Am. J. Phys. Anthropol., Suppl. *18*:48–49.

Albrecht GH (1990) Landmarks, thin plate splines, and comparative anatomy of the primate scapula. Am. Zool. *30*:73A.

Albrecht GH (1991) Thin plate splines and the primate scapula. Am. J. Phys. Anthropol., Suppl. *12*:42–43.

Atchley WR, Gaskins CT, and Anderson D (1976) Statistical properties of ratios. I. Empirical results. Syst. Zool. *25*:563–583.

Berry RJA, and Robertson AWD (1914) Dioptrographic tracings in three normae of ninety Australian aboriginal crania. Trans. R. Soc. Victoria *6*.

Blackith RE, and Reyment RA (1971) Multivariate Morphometrics. New York: Academic Press.

Bookstein FL (1986) Size and shape spaces for landmark data in two dimensions. Stat. Sci. *1*:181–242.

Bookstein FL (1989) Principal warps: Thin-plate splines and the decomposition of the deformations. IEEE Trans Pattern Analysis Machine Intelligence *11*: 567–585.

Bookstein FL (1991) Morphometric Tools for Landmark Data. Geometry and Biology. Cambridge: Cambridge University Press.

Bookstein FL (1992) A brief history of the morphometric synthesis. In Marcus LF, Bello E, and Garcia-Valdescasas A (eds): Contributions to Morphometrics. Madrid: Museo Nacional de Ciencias Naturales, pp. 18–40.

Bookstein FL (1996) Combining the tools of geometric morphometrics. In Marcus LF, Corti M, Loy A, Naylor GJP, and Slice DE (eds.): Advances in Morphometrics. New York: Plenum, pp. 131–151.

Boule M (1911–1913) L'homme fossile de la Chapelle-aux-Saints. Ann. Paleontol. *6*:111–172, *7*:21–56, 85–192, *8*:1–70.

Boule M (1921) Les hommes fossiles. Paris: Masson.

Brace CL (1964) The fate of the "classic" Neanderthals: A consideration of hominid catastrophism. Curr. Anthropol. *5*:3–43.

Brace CL (1979) Krapina, "classic" Neanderthals, and the evolution of the European face. J. Hum. Evol. *8*:527–550.

Brace CL (1981) Tales of the phylogenetic woods: The evolution and significance of evolutionary trees. Am. J. Phys. Anthropol. *58*:411–429.

Brace CL (1991) Monte Circeo, Neanderthals, and continuity in European cranial morphology, a rear end view. In Piperno M and Scichilone G (eds): Il Cranio Neanderthaliano Circeo 1. Studi e Documenti. Rome: Ministero per i Beni Culturali e Ambientali, pp. 175–195.

Brace CL (1995) The Stages of Human Evolution. 5th ed. Englewood Cliffs, N.J.: Prentice-Hall.

Brüer G (1992) Africa's place in the evolution of *Homo sapiens*. In Braher G and Smith FH (eds): Continuity or Replacement: Controversies in *Homo sapiens* Evolution. Rotterdam: Balkema, pp. 83–98.

Condemi S (1988) Caractères plésiomorphes et apomorphes de l'os temporal des néandertaliens européens whrmiens. In Trinkaus E (ed): L'homme de Néandertal, Vol. 3, L'Anatomie. Etudes et Recherches de l'Université de Liège, No. 30, pp. 49–52.

Coon CS (1962) The Origin of Races. New York: Knopf.

Coward WM, and McConathy D (1996) A Monte Carlo study of the inferential properties of three methods of shape comparison. Am. J. Phys. Anthropol. *99*:369–377.

Darroch JN, and Mosimann JE (1985) Canonical and principal components of shape. Biometrika *72*: 241–252.

Fink WL, and Zelditch ML (1995) Phylogenetic analysis of ontogenetic shape transformations. A reassessment of the piranha genus *Pygocentrus* (Teleostei). Syst. Biol. *44*.

Franciscus RG, and Trinkaus E (1995) Determinants of retromolar space presence in Pleistocene *Homo* mandibles. J. Hum. Evol. *28*:577–595.

Frayer DW (1992) Evolution at the European edge: Neanderthal and Upper Paleolithic relationships. Préhistoire Européenne *2*:9–69.

Fürst DM, and Hansen CC (1951) Crania groenlandica. A *Description of Greenland Eskimo Crania with an* Introduction on the Geography and History of Greenland. Copenhagen: Andr. Fred. Höst and Son.

Gelvin B, and Albrecht GH (1993) Morphological comparisons among hominoid ilia using thin-plate splines. Am. J. Phys. Anthropol., Suppl. *16*:93.

Gorný S (1957) Crania africana, Uganda. Wroclaw: Polska Akademia Nauk, Materialy i Prace Antropologiczne, No. 14.

Gorjanovič-Kramberger D (1960) Der Diluviale Mensch von Krapina in Kroatien: Ein Beitrag zur Paläoanthropologie. Weisbaden: Kreidel.

Groves CP (1989) A New Theory of Primate and Hominid Evolution. Oxford: Clarendon.

Heim J-L (1976) Les hommes fossiles de la Ferrassie. Arch. Inst. Paléontol. Hum., Mém. *35*.

Heim J-L (1989) La nouvelle reconstitution du crâne néandertalien de La Chapelle-aux-Saints. Bull. Mem. Soc. Anthropol. Paris *1*(1–2):95–118.

Hooton EA (1946) Up from the Ape. 2nd ed. New York: MacMillan.

Howells WW (1973) Cranial Variation in Man. A Study by Multivariate Analysis of Patterns of Difference among Recent Human Populations. Pap. Peabody Mus. Archaeol. Ethnol., Vol. 67.

Howells WW (1974) Neanderthal man: Facts and figures. Yrbk. Phys. Anthropol. *18*:7–18.

Howells WW (1989) Skull Shapes and the Map. Craniometric Analyses in the Dispersion of Modern *Homo*. Papers of the Peabody Museum of Archaeology and Ethnology, Harvard University, Volume 79.

Howells WW (1993) Getting Here: The Story of Human Evolution. Washington, D.C.: Compass.

Hrdlička A (1930) The Skeletal Remains of Early Man. Washington, D.C.: Smithsonian Institution.

Hublin J-J (1978) Quelques caractères apomorphes du crâne néandertalien et leur interprétation phylogénique. C. R. Acad. Sci. Paris, Ser. D, *287*:923–926.

Hublin J-J (1988) Caractères derivés de la région occipito-mastoïdienne chez les Néandertaliens. *In Trinkaus*

E (ed): L'homme de Néandertal, Vol. 3, L'Anatomie. Etudes et Recherches de l'Université de Liège, No. 30, pp. 67–73.

Huxley TH (1863) Man's Place in Nature. London: E.P. Dutton.

Hylander WL, Pascal GP, and Johnson KR (1991) Masticatory-stress hypothesis and the supraorbital region of primates. Am. J. Phys. Anthropol. *86:*1–36.

Jolicoeur P (1963) The multivariate generalization of the allometry equation. Biometrics *19:*497–499.

Kennedy G (1992) The evolution of *Homo sapiens* as indicated by features of the postcranium. In Bräuer G and Smith FH (eds): Continuity or Replacement: Controversies in *Homo sapiens* Evolution. Rotterdam, Balkema, pp. 209–218.

LeGros Clark WE (1978) The Fossil Evidence for Human Evolution. 3rd ed. Chicago: University of Chicago.

MacCurdy G (1924) Human Origins: A Manual of Prehistory. New York: D. Appleton.

Mahalanobis PD (1936) On the generalised distance in statistics. Proceedings of the National Institute of Science of India, Part A *2:*49–55.

Manouvrier L (1888) Mémoire sur la platcynémie chez l'homme et chez les anthropoïdes. Mém. Soc. Anthropol. Paris *3:*469–550.

Manzi G (1991) Platycephaly and encephalization in the Grotta Guattari cranium (Monte Circeo): Parieto-occipital morphology of a typical Neanderthal. In Piperno M and Scichilone G (eds): Il Cranio Neanderthaliano Circeo 1. Studi e Documenti. Rome, Ministero per i Beni Culturali e Ambientali, pp. 253–272.

Marcus LF (1990) Traditional morphometrics. In Rohlf FJ, and Bookstein FL (eds.): Proceedings of the Michigan Morphometric Workshop. University of Michigan Museum of Zoology, Special Publication No. 2, pp. 77–122.

Marcus LF, Bello E, and Garcia-Valdescasas A (eds) (1993) Contributions to Morphometrics. Madrid: Museo Nacional de Ciencias Naturales.

Marcus LF, Corti M, Loy A, Naylor GJP, and Slice DE (eds) (1996) Advances in Morphometrics. New York: Plenum.

Martin H (1926) Recherches sur l'évolution du Moustérien dans le gisement de La Quina (Charente), Vol IV, L'enfant fossile de La Quina. Paris, Librairie Octave Doin.

McCown TD, and Keith A (1939) The Stone Age of Mount Carmel. Oxford: Claredon.

Mosimann JE (1970) Size allometry: size and shape variables with characterizations of the lognormal and generalized gamma distributions. J. Amer. Stat. Assoc. *65:*930–945.

Mosimann JE and James FC (1979) New statistical methods for allometry with application to Florida redwinged blackbirds. Evol. *33:*444–459.

Morton DJ (1926) Significant characteristics of the Neanderthal foot. Nat. Hist. *26:*310–314.

O'Higgins P, and Dryden IL (1993) Sexual dimorphism in hominoids: Further studies of craniofacial shape differences in *Pan, Gorilla* and *Pongo.* J. Hum. Evol. *24:*183–205.

Patte E (1995) Les Néanderthaliens. Paris: Masson.

Pearson K, and Davin AG (1924) On the biometric constants of the human skull. Biometrika *16:*328–363.

Piperno M, and Scichilone G (eds) (1991) Il Cranio Neanderthaliano Circeo 1. Studi e Documenti. Rome: Ministero per i Beni Culturalie e Ambientali.

Ravosa MJ (1991) Interspecific perspective on mechanical and non-mechanical models of primate circumorbital morphology. Am. J. Phys. Anthropol. *86:*369–396.

Rak Y (1986) The Neanderthal: A new look at an old face. J. Hum. Evol. *15:*151–164.

Rak Y (1992) Morphological variation in *Homo neanderthalensis* and *Homo sapiens* in the Levant: A biogeographic model. In Kimbel WH and Martin LB (eds): Species, Species Concepts, and Primate Evolution. New York: Plenum, pp. 523–536.

Reyment RA (1991) Multidimensional Paleobiology. London: Pergamon Press.

Richtsmeier JT, Cheverud JM, and Lele S (1992) Advances in anthropological morphometrics. Ann. Rev. Anthropol. *21:*283–305.

Rightmire GP (1990) The Evolution of *Homo erectus.* Comparative Anatomical Studies of an Extinct Human Species. Cambridge: Cambridge University Press.

Rohlf FJ (1990) An overview of image processing and analysis techniques for morphometrics. In Rohlf FJ and Bookstein FL (eds): Proceedings of the Morphometrics Workshop. Spec. Publ. No. 2, Univ. Mich. Mus. Zool., pp. 37–60.

Rohlf FJ (1992) Relative warp analysis and its application to mosquito wings. In Marcus LF, Bello E, and Garcia-Valdescasas A (eds): Contributions to Morphometrics. Madrid: Museo Nacional de Ciencias Naturales, pp. 134–159.

Rohlf FJ, and Marcus LF (1993) A revolution in morphometrics. Trends Ecol. Evol. *8:*129–132.

Santa Luca AP (1978) A re-examination of presumed Neanderthal-like fossils. J. Hum. Evol. *7:*619–636.

Santa Luca AP (1980) The Ngandong Fossil Hominidae: A Comparative Study of a Far Eastern *Homo erectus* Group. Yale Univ. Publ. Anthropol. *75:*1–175.

Schaaffhausen D (1858) Zur Kenntnis der älteste Rassenschädel. Archiv für Anatomie, Physiologie und Wissenschaftliche Medicin, Mehreren Gelehrten herausgegeben von Dr. Johannes Müller, pp. 453–478.

Schaefer SA, and Lauder GV (1996) Testing historical hypotheses of morphological change: Biomechanical decoupling in loricarioid catfishes. Evolution *1661:* 1675.

Schreiner KE (1939) Crania norvegica. I. Instituttet for Sammenlignende Kulturforskning (Oslo), Ser. B, Skrifter *36.*

Schwalbe G (1901) Der Neanderthalschädel. Bonn. Jahrb. *106:*1–72.

Somers KM (1986) Multivariate allometry and removal of size with principal components analysis. Syst. Zool. *35:*359–368.

Somers KM (1989) Allometry, isometry and shape in principal components analysis. Syst. Zool. *38:*169–213.

Smith FH (1983) Behavioral interpretations of the changes in craniofacial morphology across the archaic/modern *Homo sapiens* transition. In Trinkaus E (ed): The Mousterian Legacy. Oxford: B.A.R. International Series 164, pp. 141–163.

Smith FH, and Paquette SP (1989) The adaptive basis of Neanderthal facial form, with some thoughts on the

nature of modern human origins. In Trinkaus E (ed): The Emergence of Modern Humans. Biocultural Adaptations in the Later Pleistocene. Cambridge: Cambridge University Press, pp. 181–210.

Sollas WJ (1908) On the cranial and facial characters of the Neanderthal race. Philos. Trans. R. Soc. Lond. [Biol]. *99:*281–339.

Sollas WJ (1924) Ancient Hunters and Their Modern Representatives. 3rd ed. New York: MacMillan.

Spencer MA, and Demes B (1993) Biomechanical analysis of masticatory system configuration in Neanderthals and Inuits. Am. J. Phys. Anthropol. *91:*1–20.

Stewart TD (1962) Neanderthal cervical vertebrae. Bib. Primat. *1:*130–154. Basel/New York: S. Karger.

Straus WL Jr, and Cave AJE (1957) Pathology and the posture of Neanderthal man. Q. Rev. Biol. *32:*348–363.

Stringer CB, and Andrews P (1988) Genetic and fossil evidence for the origin of modern humans. Science *239:*1263–1268.

Stringer C, and Gamble C (1993) In Search of the Neanderthals. London: Thames and Hudson.

Stringer CB, Howell, FC, and Melentis JK (1979) The significance of the fossil hominid skull from Petralona, Greece. J. Archaeol. Sci. *6:*253–254.

Stringer CB, Hublin J-J, and Vandermeersch B (1984) The origin of anatomically modern humans in Western Europe. In Smith FH and Spencer F (eds): The Origins of Modern Humans. New York: Alan R. Liss, pp. 51–135.

Suzuki H, and Takai F (eds) (1970) The Amud Man and His Cave Site. Tokyo: Academic.

Swiderski D (1993) Morphological evolution of the scapula in tree squirrels, chipmunks, and ground squirrels (Sciuridae): An analysis using thin-plate splines. Evolution *47:*1854–1873.

Tabachnick R, and Bookstein FL (1990) Resolving factors of landmark deformation: Miocene *Globorotalia* DSDP site 593. In FJ Rohlf and FL Bookstein (eds): Proceedings of the Michigan Morphometrics Workshop. University of Michigan Museum of Zology: Spedial Publication No. 2. Ann Arbor, Michigan, pp. 269–281.

Thompson D'A (1917) On Growth and Form. Cambridge: Cambridge University Press.

Thorne AG, and Wolpoff MH (1981) Regional continuity in Australian Pleistocene hominid evolution. Am. J. Phys. Anthropol. *55:*337–349.

Trinkaus E (1983) The Shanidar Neanderthals. New York: Academic.

Trinkaus E (1984) Western Asia. In Smith FH and Spencer F (eds): The Origins of Modern Humans. New York: Alan R. Liss, pp. 251–293.

Trinkaus E (1987) The Neanderthal face: Evolutionary and functional perspectives on a recent hominid face. J. Hum. Evol. *16:*429–443.

Trinkaus E (1988) The evolutionary origins of the Neanderthals, or why were there Neanderthals? In Trinkaus E (ed): L'homme de Néandertal, Vol. 3, L'Anatomie. Etudes et Recherches de l'Université de Liège, No. 30, pp. 11–29.

Trinkaus E, Arter DD, and Franciscus RG (n.d.) A reconstruction of the Shanidar 4 facial skeleton, and a reconsideration of the evolutionary emergence of the Neanderthal face. J. Human Evol., in press.

Trinkaus E, and Howells WW (1979) The Neanderthals. Sci. Am. *241*(6):118–133.

Trinkaus E, and LeMay M (1982) Occipital bunning among later Pleistocene hominids. Am. J. Phys. Anthropol. *57:*27–35.

Vandermeersch B (1989) The evolution of modern humans: Recent evidence from Southwest Asia. In Mellars P and Stringer C (eds): The Human Revolution: Behavioural and Biological Perspectives on the Origins of Modern Humans. Princeton, N.J.: Princeton University Press, pp. 155–164.

von Luschan F (1907) Sammlung Baessler. Schädel von polynesischen Inseln, gesammelt und nach dem Fundorten beschriebon von Arthur Baessler. Berlin: G. Reimer.

Willermet CM (1994) Craniometric data and phylogenetic issues in human evolution. Poster Presentation at the 63rd Annual Meeting of the Am. Assoc. Phys. Anthropol., Denver, Colorado, March 31, 1994.

Wolpoff MH (1980) Paleoanthropology. New York: Knopf.

Wolpoff MH, Smith FH, Malez M, Radovčić J, and Rukavina D (1981) Upper Pleistocene remains from Vindija Cave, Croatia, Yugoslavia. Am. J. Phys. Anthropol. *54:*499–544.

Wolpoff MH (1992) Theories of modern human origins. In Braüer G and Smith FH (eds): Continuity or Replacement: Controversies in *Homo sapiens* Evolution. Rotterdam: Balkema, pp. 25–63.

Yaroch LA (1994a) Characterization of Neanderthal Cranial Shape Using the Method of Thin-Plate Splines. Ph.D. dissertation, University of Michigan.

Yaroch LA (1994b) Neanderthal facial shape and masticatory muscle position: An investigation using thin-plate splines. Am. J. Phys. Anthropol., Suppl. *18:*212.

Yaroch LA (1995) An atypical Neanderthal: Cranial shape in the "old man" from La Chapelle-aux-Saints. Am. J. Phys. Anthropol., Suppl. *20:*225.

Yaroch LA (n.d.) An atypical Neanderthal: Cranial shape in the "old man" from La Chapelle-aux-Saints. Unpublished manuscript.

Zelditch ML, Bookstein FL, and Lundrigan B (1992) Ontogeny of integrated skull growth in the cotton rat *Sigmodon fulviventer.* Evolution *46:*1164–1180.

Zelditch ML, Bookstein FL, and Lundrigan B (1993) The ontogenetic complexity of developmental constraints. J. Evol. Biol. *6:*621–641.

Zelditch ML and Fink WL (1995) Allometry and developmental integration of body growth in a piranha, *Pygocentrus nattereri* (Teleostei: Ostariophysi). J. Morphol. *223:*341–355.

Zelditch ML and Fink WL (1997) Shape analysis and taxonomic status of *Pygocentrus* piranhas (Ostariophysi, Characiformes) from the Paraguay and Paran river basin of South America. Copeia, in press.

Zelditch ML, Fink WL, and Swiderski DL (1995) Morphometrics, homology, and phylogenetics: Quantified characters as synapomorphies. Syst. Biol. *44:*179–189.